

Functionalization and rehabilitation applications of sodium alginate-based hydrogels

Zixuan Meng^{1#}, Xinpeng Wang^{2#*}, Yingying He³, Kangming Tian^{1*}, Jinlai Miao^{3*}, and Yubo Fan^{2,4}

ABSTRACT

Sodium alginate (SA)-based hydrogels, derived from SA, are a class of polymer hydrogels that have garnered significant attention due to their excellent biocompatibility, eco-friendly production processes, and the abundance and cost-effectiveness of their raw materials. These hydrogels hold vast potential for applications across multiple fields, such as biomedical engineering, flexible sensors, food science, and environmental management. To enhance and diversify their functional capabilities, the functionalization of SA-based hydrogels has become a focal point of research. This study provides a comprehensive review of the field, starting with a systematic summary of the functional preparation methods of SA-based hydrogels developed in recent years. These methods encompass physical and chemical modification techniques, which are crucial for tailoring the properties of the hydrogels to specific applications. Physical modification is typically achieved by mixing with nanomaterials, natural materials, and polymer materials through physical interaction forces, whereas chemical modification is mainly obtained through oxidation, sulfonation, and graft polymerization. The main applications of SA-based hydrogels are also reviewed, including those applied in flexible detection, tissue engineering, food, and water treatment, offering a detailed comparative analysis of their performance in these areas. Finally, the study looks ahead to future research and development prospects of SA-based hydrogels, aiming to drive further advancements in their functional development and expand their application scope. By thoroughly analyzing current research and future directions, this paper seeks to stimulate continued innovation and practical applications of SA-based hydrogels.

Keywords:

Sodium alginate; Hydrogel; Functionalization; Biomedical engineering

#Authors contributed equally.

*Corresponding author:

Xinpeng Wang,
wangxinpeng@uhrs.edu.cn;
Kangming Tian,
kangmingtian@tust.edu.cn;
Jinlai Miao,
miaojinlai@fio.org.cn

How to cite this article:

Meng Z, Wang X, He Y, Tian K, Miao J, Fan Y. Functionalization and rehabilitation applications of sodium alginate-based hydrogels. *Biomater Transl.* 2026, 7(2), 201-227.

doi: [10.12336/bmt.25.00006](https://doi.org/10.12336/bmt.25.00006)



1. Introduction

Hydrogels, soft materials featuring a three-dimensional (3D) architecture, exhibit tunable physicochemical characteristics.¹⁻³ Its raw materials are hydrophilic polymers, including natural hyaluronic acid, alginate, pectin, chitosan (CS), gelatin, collagen, fibrin, pectin, and sulfate, as well as artificially synthesized polyethylene oxide, polyethylene glycol, and polyvinyl alcohol (PVA). Notably, sodium alginate (SA) arises chiefly as a secondary product during iodine and mannitol extraction from brown algae such as kelp. It is a linear natural polysaccharide polymer composed of β -1,4-D-mannuronic acid units and α -1,4-L-guluronic acid units,⁴ as shown in **Figure 1**. It is derived from a wide range of sources at a low cost. The hydrogel prepared by SA has

excellent biocompatibility, an environmentally friendly preparation process, and low cost. It has great potential for application in biomedical engineering, food, environment, and other fields.

Hydrogels are often functionalized to meet specific application needs to enhance the functionality or characteristics of SA, such as improving mechanical properties, biocompatibility, environmental responsiveness, conductivity, and adhesion.⁵ In recent years, the development of functionalized SA-based hydrogels has expanded their applications across various fields, such as flexible sensing, tissue engineering, environment, and food industries.⁶⁻⁸

This paper provides an overview of recent advancements in the functionalization and application of SA-based hydrogels. It examines

the modifications and functionalization these hydrogels have undergone in recent years. It then delves into their applications across different fields, highlighting their unique characteristics. Finally, based on the current state of research, the paper discusses potential future directions for SA-based hydrogels, aiming to encourage further research into their functionalization and uses.

2. Preparation and functionalization of SA-based hydrogel

SA-based hydrogels, a versatile alginate polymer, are predominantly synthesized through various cross-linking techniques, encompassing ionic, covalent, free radical polymerization, and cell-based methods. Among these, ionic cross-linking is the most prevalent approach, which entails mixing an SA solution with ionic agents such as calcium ions (Ca^{2+}) or gallium ions,^{9,10} facilitating gel formation under relatively mild conditions.¹¹ Covalent cross-linking, in contrast, establishes robust bonds between polymer chains through reactions such as amide formation,¹² Schiff base,¹³ condensation,¹⁴ or addition, allowing the production of blended hydrogels with precise control over degradation rates and mechanical properties.¹⁵ Free radical polymerization cross-linking integrates polymerizable groups into water-soluble polymers, which subsequently undergo chemical cross-linking through radical copolymerization in the presence of a cross-linking agent.¹⁶ Moreover, the SA-based hydrogel formed through cell cross-linking does not require chemical reagents. It links the alginate polymer chain with the cell adhesion peptide to form a uniform solution and ultimately forms a reversible network structure through specific receptor-ligand interaction.¹⁷

In general, the enhancement of SA-based hydrogels involves both physical and chemical modification techniques, as depicted in **Figure 2**. These modifications are designed to optimize the hydrogels' properties, ensuring they excel in targeted applications.

2.1. Physical modification

Physical modification is one of the most straightforward, cost-effective, and practical strategies for creating new polymer composite materials.¹⁸ The molecular structure of SA contains abundant hydroxyl and carboxyl groups, which can easily form physical interactions with functional groups of various polymers. This process significantly boosts the material's mechanical properties. Moreover, during the mixing phase, the inherent qualities of these polymers are preserved, effectively addressing many of the limitations associated with SA-based hydrogels. At present, enhancements to the properties of SA are predominantly achieved via physical modification and

functionalization, often involving blending with nanomaterials, natural biomaterials, and synthetic polymer materials.¹⁹ The classification and advantages of SA-based hydrogel functionalized through physical modification are summarized in **Table 1**. The physical modification method primarily relies on intermolecular force, enhancing biocompatibility, though its poor mechanical properties limit its use to non-mechanical applications. However, the mechanical and electrical properties are enhanced by incorporating more physical interactions in the design. These advancements pave the way for developing SA-based hydrogels with improved properties, broadening their potential applications in various fields.

2.1.1. Blending with nanomaterials

Nanomaterials, with their diverse capabilities, remarkable porosity, and sky-high surface-area-to-volume ratio, can form these fascinating, interconnected nanofiber webs when mixed with SA.¹⁰ This blending method allows SA to demonstrate advantages in many applications.

- (i) Introducing nanoparticles can enhance SA-based hydrogels' mechanical properties. For example, adding hydroxyapatite (HA) nanoparticles can significantly improve the compression strength of SA-based hydrogels⁴⁶
- (ii) The dynamic cross-linking capability of nanoparticles, such as silver and montmorillonite, interacts with the carboxyl group of SA to form a multiple cross-linking mechanism. This enhances the stability of hydrogel under different pH or ionic environments⁴⁷
- (iii) In terms of drug delivery, the introduction of nanoparticles has changed hydrogels' porosity and hydrophilic hydrophobic balance to achieve precise control of drug release. For example, the encapsulation efficiency of SA-based hydrogels loaded with montmorillonite nanoparticles for favipiravir has been improved to more than 80%, and the release kinetics conforms to the Super Case II model, meaning the drug release rate is dominated by the relaxation of the polymer chain, rather than simple diffusion⁴⁸
- (iv) Regarding biological activity, a few nanoparticle-modified SA-based hydrogels can induce bone formation, which is suitable for bone tissue engineering. At the same time, the modified gel can also promote cell adhesion, which is very important for biomedical applications.

Nanoparticle modification has upgraded SA-based hydrogel from a single biomaterial to an intelligent, responsive platform through multiscale structure regulation and functional module integration, showing irreplaceable advantages in tissue engineering (bone repair and skin regeneration), environmental governance (heavy metal adsorption), food industry (lubricant and fat replacement) and other fields. For example, Li *et al.*⁴⁹ took a clever

¹Department of Biological Chemical Engineering, College of Chemistry Engineering and Materials Science, Tianjin University of Science and Technology, Tianjin, China; ²Biomechanics and Health Engineering Laboratory, School of Rehabilitation Sciences and Engineering, Qingdao Central Hospital, University of Health and Rehabilitation Sciences, Qingdao, Shandong, China; ³Qingdao Key Laboratory of Marine Natural Products R&D Laboratory, First Institute of Oceanography, Ministry of Natural Resources, Qingdao, Shandong, China; ⁴Key Laboratory for Biomechanics and Mechanobiology, Beijing Advanced Innovation Center for Biomedical Engineering, School of Biological Science and Medical Engineering, Beihang University, Beijing, China

approach, using hydrogen bonding to crosslink silk fibroin-modified carbon nanotubes into a matrix of SA and PVA, as illustrated in **Figure 3A**. The resulting hydrogel boasted a tensile strength of 120 KPa at the breaking point and a self-healing capability that patched up 67.2% of fractures. As a strain sensor, it could detect even the slightest tweak-down to a mere 0.5% strain and showed a gauge factor of 4.75 across a 0 – 17% range. This opens up possibilities for using hydrogel in all portable and wearable gadgets. By leveraging carbon nanotubes that are non-covalently modified, the hydrogel's

resilience and responsiveness are enhanced. This innovative hydrogel design converts external stimuli, such as pressure or strain, into real-time electrical signals, highlighting its potential as a high-performance sensor. To illustrate, the team utilized delignified wood as the structural scaffold and then intricately integrated polyacrylamide (PAM) and SA into this framework. The final touch was the incorporation of multiwalled carbon nanotubes (CNTs), which significantly enhanced the material's electrical conductivity. This synergistic combination endowed the hydrogel with remarkable mechanical strength (tensile strength of 13.7 MPa) and exceptional durability, allowing it to withstand repeated bending without degradation. The addition of CNTs also supercharged its electrochemical capabilities, resulting in a specific capacitance of 211.2 mF/cm² (at 1 mA/cm²) when used as a supercapacitor with an impressive ionic conductivity of 74.9 mS/cm.⁵⁰ This preparation technique offers an inventive and hopeful approach to creating robust bio-based hydrogel electrolytes with promising uses across various industries. Incorporating multiwalled carbon nanotubes and graphene nanosheets (GNPs) will improve osteogenic differentiation and the structural and mechanical characteristics of scaffolds utilized in bone tissue engineering. Seifi *et al.*⁵¹ enhanced scaffold performance by loading PVA, CS, and SA composites with CNTs and GNPs. It has been proved that this cocktail significantly increased conductivity and stiffness. In addition, they observed a 36% improvement in the activity of human osteosarcoma cells (MG63) osteoblasts by adding CNTs

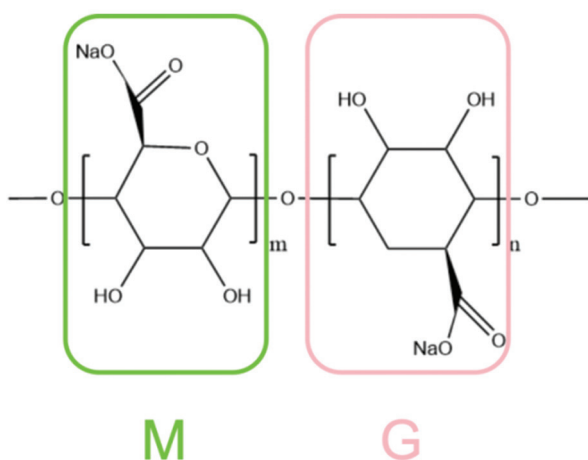


Figure 1. Sodium alginate structural formula M refers to β -1,4-D-mannuronic acid, and G refers to α -1,4-L-guluronic acid.

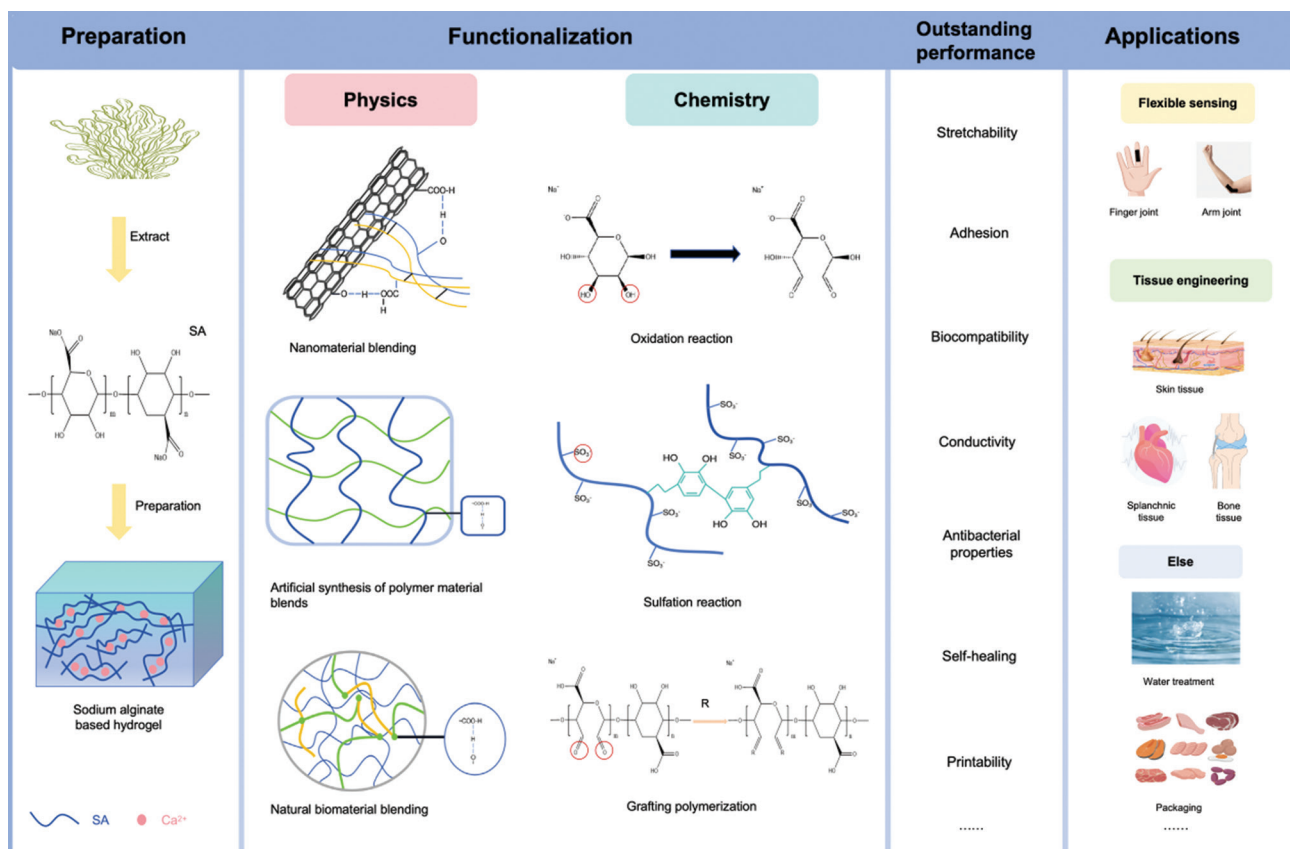


Figure 2. Functionalization and application of sodium alginate-based hydrogel. Image created from Freepik.com. Abbreviation: SA: Sodium alginate.

Table 1. Functionalization (physical modification) and application of sodium alginate-based hydrogel

Sodium alginate content	Other components	main Interactions	Functionalization	Advantages	Applications	References
100 mg/mL	Zinc cyclic dinucleotide, phenylboronic acid, and indocyanine green	Metal coordination bond	Nanomaterial blending	Biocompatibility, drug delivery (cyclic dinucleotide and manganese ions), and light induction	Tumor treatment	9
7 wt%	Thiocarboxymethyl chitosan	Electrostatic force	Natural biomaterial blending	Adhesive properties, hemostatic properties, biocompatibility	Wound healing	13
2 wv%	Carboxymethyl chitosan	Electrostatic force	Natural biomaterial blending	Antibacterial activity, biocompatibility, antithrombotic activity (<i>Escherichia coli</i> and <i>Staphylococcus epidermidis</i>)	Blood contact equipment	20
2 wt%	Polyvinyl alcohol	Hydrogen bond	Artificial polymer material blending	Adhesion (75.08 kPa), antibacterial (<i>E. coli</i>), biocompatibility	Adhesive	21
1 wt%	Polyvinyl alcohol, diethanolamine, calcium phosphate, alkaline phosphatase	Hydrogen bond	Artificial polymer material blending	Stretchability (elastic modules 103 MPa), anti-swelling, high toughness (1.86 MJ/m ³), biocompatibility, osteogenic ability	Bone repair	22
/	Urea, zinc ions	Metal coordination bond	Natural biomaterial blending	Biocompatibility, sensing, cycling stability, flexibility	Flexible electronics	23
1 wt%	Titanium carbide, glycine	Hydrogen bond, electrostatic force	Nanomaterial blending	Strong stretchability (>5,000%), water retention (>30 days), sensing (gauge factor of 29.3)	Flexible electronics	24
1.09 wt%	Chitosan, calcium carbonate	Electrostatic force	Natural biomaterial blending	Strong mechanical properties (elastic modules 40 kPa), swelling ability (4,500%), biocompatibility	Bone repair	25
3 wt%	Quaternized chitosan	Electrostatic force	Natural biomaterial blending	Printability, self-healing, biocompatibility, antibacterial properties (<i>E. coli</i> and <i>Staphylococcus aureus</i>)	Wound healing	26
5 mg/mL	Hyaluronic acid	Hydrogen bond	Natural biomaterial blending	Drug delivery (doxorubicin), biocompatibility, biodegradability	Drug delivery	27
/	Silica calcium nanowire	Ionic bond	Nanomaterial blending	Printability, strong mechanical properties (elastic modules 14.84 kPa), osteogenic differentiation	Bone repair	28
/	Gelatin methacrylate, black phosphorus nanosheets	Electrostatic force, hydrogen bond	Nanomaterial blending	Biocompatibility, promotion of osteogenesis, induction of cell differentiation, drug delivery (deferaxamine)	Bone repair	29
12 mg/mL	Reduced graphene oxide	Hydrogen bond	Nanomaterial blending	Salt resistance, excellent evaporation rate (4.13 kg·m ⁻² /h)	Seawater desalination	30
3 wt%	Huangqi gum, methylcellulose, aloe vera	Hydrogen bond	Natural biomaterial blending	Swelling, degradability, stretchability (Tensile strength 68.25 MPa), water resistance	Packaging	31
20 mg/mL	Silicon nanofibers, reduced graphene oxide	Hydrogen bond	Nanomaterial blending	Moisture absorption capacity (1.16 g/g), conductivity (1.46 S/m), environmental adaptability	Wet energy conversion	32

(Cont'd...)

Table 1. (Continued)

Sodium alginate content	Other components	main	Interactions	Functionalization	Advantages	Applications	References
1.5 wt%	Polyacrylamide, polypyrrole nanospheres		Hydrogen bond	Nanomaterial blending	Stretching (tensile strength of 560 kPa at 870%), self-healing, conductivity (6.44 S/m)	Flexible electronics	33
/	Glycyrrhetic acid, zinc ions		Metal coordination bond	Nanomaterial blending	Drug delivery (lonidamine), biocompatibility, regulation of inflammatory environment	Inflammation treatment	34
10 wv%	Cold water fish skin gelatin		Electrostatic force	Natural biomaterial blending	Printability, biocompatibility, biodegradability, promotion of osteogenesis	Bone repair	35
2 wv%	Illismote copper, galactose		Electrostatic force	Natural biomaterial blending	Enhance the effectiveness of tumor radiotherapy, anti-tumor immune response, and drug delivery (elesclomol-copper ions)	Cancer treatment	36
1 wv%	Chlorella, calcium ions		Electrostatic force	Natural biomaterial blending	pH response, biodegradability, biocompatibility, drug delivery (insulin)	Drug delivery	37
0.1 wt%	Methacrylate bovine serum albumin, liquid metal		Electrostatic force	Natural biomaterial blending	Large sensing and detection range (10 pg/mL – 100 ng/mL), strong sensitivity	Flexible electronics	38
6 wt%	Thymol, tannic acid, polylysine		Electrostatic force	Artificial polymer material blending	Antibacterial (<i>E. coli</i> and <i>S. aureus</i>), biocompatible, wide pH (4 – 9) response range	Wound healing	39
/	Polydopamine nanoparticles, calcium phosphate		Hydrogen bond	Artificial polymer material blending	Printability, pH response, drug delivery (anti-BRAF small interfering RNA), photothermal effect	Tumor treatment	40
2 wt%	Polyacrylamide		Hydrogen bond	Artificial polymer material blending	Conductivity (82.1 mS/cm), high mechanical strength (Tensile strength 563.2 kPa), cyclic stability (10,000 times)	Flexible electronics	41
1 wv%	Phenylboronic acid, polyvinyl alcohol		Hydrogen bond	Artificial polymer material blending	Printability, biocompatibility, high viscosity (25000 mPa-s)	Intraocular fillers, glass substitutes	42
20 mg/mL	Polyvinyl alcohol		Hydrogen bond	Artificial polymer material blending	High mechanical strength (>1,200%), conductivity (3.61 S/m), self-healing ability	Flexible electronics	43
2 wt%	Acrylamide		Hydrogen bond	Artificial polymer material blending	Strong sensitivity, sensing, cycling stability (2,000 times), adhesion, temperature sensitivity (22 – 100°C)	Flexible electronics	44
3 wt%	Polyvinyl alcohol, gelatin		Hydrogen bond	Artificial polymer material blending	Antibacterial (<i>S. aureus</i>), high mechanical strength (tensile modules 445 kPa), biocompatibility, biodegradability, drug delivery (tea polyphenol self-assembled magnesium nanoparticles)	Wound healing	45

Note:/refers to no information available.

Abbreviations: wt%: Weight percent; wv%: Weight per volume.

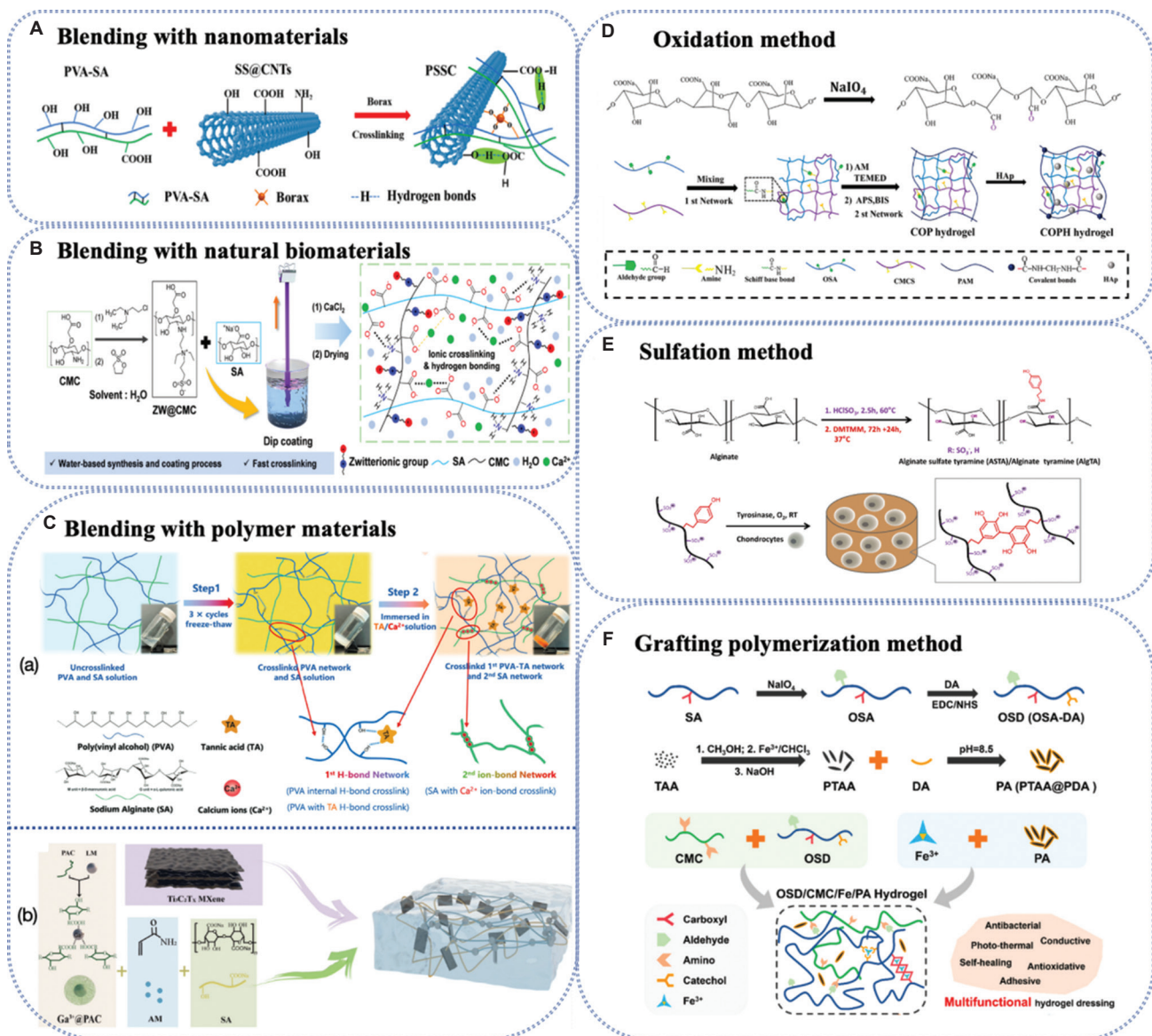


Figure 3. Preparation diagram of sodium alginate-based hydrogels functionalized. (A-C) physical modification methods: Blending with nanomaterials,⁴⁹ blending with natural biomaterials,²⁰ and blending with artificially synthesized polymer materials (PVA (a),²¹ LM (b)⁶⁰), respectively. (D-E) Chemical modification methods: oxidation method,⁶¹ sulfation method,⁶² and grafting polymerization method.⁶³ (A) Image used with permission from Elsevier Ltd, Copyright © 2022, Elsevier Ltd.⁴⁹ (B) Image used with permission from Elsevier B.V., Copyright © 2023, Elsevier B.V.²⁰ (Ca) Image used with permission from Wiley-VCH GmbH, Copyright © 2024, Wiley-VCH GmbH.²¹ (Cb) Image used with permission from Elsevier B.V., Copyright © 2024, Elsevier B.V.⁶⁰ (D) Image used with permission from MDPI, Copyright © 2023, MDPI.⁶¹ (E) Image used with permission from IOP Publishing Ltd, Copyright © 2020, IOP Publishing Ltd.⁶² (F) Image used with permission from Elsevier B.V., Copyright © 2023, Elsevier B.V.⁶³

Abbreviations: AM: Acrylamide; APS: Ammonium persulfate; BIS: Bisacrylamide; CMC and CMCS: Carboxymethyl chitosan; DA: Dopamine; HAp: Hydroxyapatite; LM: Liquid metal; OSA: Oxidized sodium alginate; OSD: OSA-DA; PAC: Polyanionic cellulose; PAM: Polyacrylamide; PDA: Polydopamine; PTAA: Poly(thiophene-3-acetic acid); PSSC: Polyvinyl alcohol/sodium alginate/sericin-modified carbon nanotubes; PVA: Polyvinyl alcohol, SA: Sodium alginate; SS@CNTs: Sericin-modified carbon nanotubes; ZW@CMC: Zwitterionic carboxymethyl chitosan.

into the cocktail. These PVA/CS/SA hydrogels, with the addition of CNTs and GNPs, show potential in bone tissue engineering.

2.1.2. Blending with natural biomaterials

Natural biomaterials, particularly biopolymers, exhibit remarkable compatibility, inherent safety, and strong cell adhesion properties.⁵² By combining SA with other biocompatible natural materials, we can significantly boost the ability of cells to

proliferate and migrate. These natural compounds usually consist of functional groups such as hydroxyl, carboxyl, and amino groups. These functional groups can be linked to hydroxyl and carboxyl groups in SA, enhancing the hydrogel’s 3D structure and improving the mechanical properties of hydrogels using SA. In soft-tissue engineering, SA is often mixed with other biocompatible materials such as agarose, CS, hyaluronic acid, gelatin, collagen, and fibrin, which can exhibit pH sensitivity and environmental responsiveness.⁵³ This characteristic makes

it suitable as a drug delivery carrier to avoid damaging the active part. In addition, the raw material of SA-based hydrogel is derived from brown algae, which is naturally non-toxic and biocompatible. The gel modified with natural biomaterials, whose degradation products can be discharged through the kidney, will not cause an inflammatory reaction. In wound healing, the modified alginate hydrogel can simulate the humid environment of the extracellular matrix (ECM) and promote the migration of fibroblasts and angiogenesis.⁵⁴ For example, Lee *et al.*²⁰ presented an innovative approach to synthesizing zwitterionic carboxymethyl CS (CMC), employing biodegradable CMC as a hydrogel coating that offers antithrombotic and antibacterial properties (**Figure 3B**). This innovative method is different from traditional CMC coating methods, as it utilizes the inherent antibacterial properties of CMC to combat bacterial infections effectively, inhibiting the formation of contaminated hydration layers. The distinctive attributes of zwitterionic CMC render it an exceptionally advantageous biocompatible coating material, holding great promise for application across a wide spectrum of medical devices. Lee *et al.*'s research is significant in propelling the development of blood-contacting devices tailored for treating vascular disorders while substantially mitigating the risks associated with infection, thrombosis, and friction-induced vascular injuries. Furthermore, the composite hemostatic hydrogel, formulated from CMC and SA, exhibits a porous network structure that facilitates superior water absorption. It also has a low hemolysis rate and demonstrates robust *in vitro* coagulation-promoting activity. *In vivo*, hemostasis experiments showed that incorporating CMC significantly reduced blood loss and bleeding time after liver and tail injury in mice. These findings underscore the hydrogel's potential as an effective, user-friendly, and rapid-acting hemostatic agent characterized by strong safety.⁵⁵

Zhang *et al.*⁵⁶ introduced an innovative food preservation method by developing a curcumin/SA/CMC hydrogel (CSCH) matrix. The team successfully engineered a 3D network that efficiently encapsulates curcumin by capitalizing on the inherent electrostatic interactions between oppositely charged polysaccharides. The results showed that the CSCH matrix enhanced the chemical stability of curcumin by more than 400% compared to its unencapsulated state and exhibited exceptional performance in gas barrier protection, antimicrobial activity, antioxidant properties, and overall safety for biological systems. This pioneering work holds significant promise for advancing food preservation technologies. Expanding on this foundational research, Xu *et al.*⁵⁷ further advanced the concept by showing that CSCH membrane demonstrated remarkable efficacy when applied to mangoes. It significantly curtailed moisture and nutrient loss, inhibited microbial growth, and decelerated respiration rates. Consequently, the fruit preserved its quality for an extended period of 11 days. Moreover, the membrane showed rapid recovery capabilities within 10 min and underwent natural degradation in 53 days, underscoring its environmentally friendly nature.

2.1.3. Blending with artificially synthesized polymer materials

In addition to the natural biomaterials discussed previously, a diverse array of synthetic polymers is often synergistically

combined with SA to augment its functional attributes. Prominent examples encompass PVA,²¹ polylactic acid (PLA),⁵⁸ and polyethylene glycol,⁵⁹ among other innovative materials. These polymers are known for their superior mechanical strength, and when blended with SA, they can significantly enhance the performance of the resulting hydrogel.²² Its classic physical cross-linking mode is the "egg box" model formed by the controllable SA of the cross-linking network through divalent cations (such as Ca²⁺). After introducing synthetic polymers such as PVA and PAM, a dual network structure can be formed through chemical cross-linking. This composite cross-linking mechanism greatly improves the porosity of the hydrogel and meets the penetration requirements of different applications. In addition, synthetic polymer materials can also endow SA-based hydrogels with certain intelligent response abilities. For example, adding temperature-sensitive materials to modify hydrogels can significantly change the swelling rate of hydrogels with temperature, which is of great value in drug delivery. In addition, synthetic polymer materials can enhance SA-based hydrogels, enabling multifunctional integration, such as adsorption, antibacterial, and electrical activity. This transformation allows SA-based hydrogels to evolve from a single functional material to one with intelligent response, high strength, and adaptability across various applications, especially in fabric repair and environmental governance, showing irreplaceable advantages.

In a groundbreaking study, Ding *et al.*⁵⁸ created an innovative wound dressing that mirrors the properties of human skin. The team engineered a smart bandage combining SA and PLA, demonstrating remarkable responsiveness to moisture changes with 99% sensitivity and a lightning-fast reaction time of 0.6 s. This design utilizes a waterproof PLA film reinforced with silver phosphate as a protective appearance, which has its unique advantages. Research results showed that it has an inhibitory effect on 99.99% of bacteria. The dressing's outer layer doubles as an extraordinarily sensitive pressure detector, with a sensitivity of 199.22 kPa⁻¹ at 0–1 kPa. It showed impressive resilience, maintaining performance through 1,500 usage cycles. Real-world testing revealed that the dressing prevented infections and stimulated blood vessel growth and skin regeneration, significantly improving wound recovery times. This innovative smart dressing with flexible sensors, advanced control systems, and seamless Bluetooth connectivity represents a groundbreaking leap in modern medical technology. It facilitates the precise and real-time monitoring of the wound healing process, allowing early detection of potential complications and timely intervention.

To achieve a balanced regulation of cohesion and adhesion, Song *et al.*²¹ developed an innovative double-network (DN) hydrogel adhesive using a two-phase method (**Figure 3Ca**). In the initial phase, a rigid hydrogel network is formed from PVA through three freeze-thaw cycles, establishing robust hydrogen bonds. In the subsequent phase, natural polyphenol tannic acid is introduced to enhance the adhesive properties of the PVA network. Simultaneously, a second, more flexible network composed of SA is crosslinked using Ca²⁺, significantly

bolstering the structural integrity of the DN hydrogel adhesive. By meticulously adjusting the PVA-to-SA ratio, an optimal balance between stickiness and strength is achieved, enhancing the hydrogel's adhesive performance. This newly developed DN hydrogel exhibits a threefold increase in adhesive strength, and the incorporation of tannic acid imparts antibacterial properties, making it a promising candidate for clinical applications.

In addition, Lou *et al.*⁶⁰ introduced an advanced composite conductive hydrogel strain sensor, demonstrating remarkable sensitivity and exceptional tensile strength. They mixed titanium carbide (MXene) and liquid metal conductive filler. They encapsulated them into DN hydrogel composed of SA and PAM, finally creating an efficient structure through hydrogen bonding (**Figure 3Cb**). This innovative approach capitalizes on the conductive prowess of two-dimensional MXene and zero-dimensional liquid metal, seamlessly integrated into the DN hydrogel framework. The MXene sheets act as a conductive adhesive, bridging the liquid metal and enhancing interfacial synergy while significantly reducing hysteresis. The strain sensor constructed from this composite DN hydrogel has high sensitivity (with a strain coefficient reaching 12.84), a broad detection range (0% – 1,500%), a quick response time (262 ms), and outstanding repeatability and stability. Results indicated this innovative hydrogel's suitability in creating flexible, wearable sensors for detecting physiological pressures.

2.2. Chemical modification

Altering SA through chemical modification involves strategically modifying its accessible hydroxyl and carboxyl groups. This process results in SA derivatives with significantly altered physical, chemical, and biochemical properties, including changes in solubility and hydrophobicity. Common methods for chemically modifying SA include oxidation, sulfation, and grafting.⁶⁴ These modifications can enhance the performance of SA-based hydrogels in various applications. As shown in **Table 2**, the classification and advantages of SA-based hydrogels functionalized by chemical modification are summarized. Typically, there has been extensive research on chemical modification via graft polymerization, which has demonstrated excellent mechanical properties and biocompatibility. These properties can be tailored to meet the requirements of many applications, such as biomedical engineering for bone repair, wound healing, and flexible electronics. Oxidation can improve mechanical strength and tailor degradation rates, making the hydrogels suitable for applications requiring specific mechanical properties. Modification through sulfation is relatively rare, possibly due to the difficulty of controlling biocompatibility during the reaction process. It could be used in gingival tissue engineering. These chemical modifications improve the intrinsic properties of SA and expand its potential applications in biomedical engineering, environmental management, and material science. We can foster the development and utilization of SA-based hydrogels in diverse domains by addressing these challenges.

2.2.1. Oxidation method

The oxidation technique is the most prevalent method for chemically modifying SA. The SA-based hydrogel modified

by oxidation reaction shows significant characteristics and advantages in structure and function. Its core lies in the molecular chain reorganization and reaction site increase brought by chemical modification, thus optimizing the physical and chemical properties of traditional SA. Molecular structure changes and the introduction of functional groups in oxidation reactions usually use oxidants such as sodium periodate to selectively break the C2 – C3 bonds of mannuronic acid and guluronic acid units in the SA molecular chain, generating oxidation products with aldehyde and carboxylic acid groups, as illustrated in the oxidation reaction section of **Figure 2**. Several benefits emerge when we compare oxidized SA-based hydrogels to their unoxidized counterparts.

- (i) As a cross-linking network is formed between the aldehyde group and other molecules, the mechanical strength and elasticity of the hydrogel will be significantly enhanced
- (ii) The oxidation process helps diminish the potential physiological toxicity associated with SA, thereby enhancing the biocompatibility of the hydrogels
- (iii) The presence of aldehyde groups in the molecular structure of oxidized SA (OSA) facilitates the creation of dynamic chemical bonds, which impart self-healing capabilities to the hydrogel, allowing it to repair itself after incurring damage
- (iv) OSA can be designed as a hydrogel responsive to physiological signals, making adaptive responses according to changes in pH and temperature to achieve intelligent control of the release mechanism
- (v) These hydrogels create a more favorable environment for cell adhesion and proliferation, ultimately aiding tissue regeneration.⁷⁸

By precisely regulating the chemical structure and cross-linking mechanism of SA, oxidative modification endows the hydrogel with degradability, self-healing, and multifunctional responsiveness, making it exhibit an application potential unmatched by traditional materials in biomedicine and environmental governance. Lei *et al.*¹³ detailed the development of a two-component *in situ* hydrogel, ingeniously crafted from maleimide-OSA and sulfhydryl CMC. This innovative hydrogel leverages the unique chemistries of its components to form a robust and versatile material, showcasing potential applications in biomedical engineering and beyond. This hydrogel exhibited a rapid gelling time, remarkable tissue adhesion, impressive hemostatic capabilities, and excellent biocompatibility. Findings indicated that the hydrogel's adhesion to tissue surpassed that of traditional fibrin glue. The material's self-repairing properties were evaluated using a rheometer in an alternating step strain scanning mode, revealing that the structure sustained damage at a 300% strain (where storage modulus G' was less than loss modulus G'') but was able to recover under a 1% strain (where G' exceeded G''). The hydrogel demonstrated a cycle of reconstruction and destruction when subjected to oscillating strains between 1% and 300%, showcasing its commendable self-healing abilities. Geng *et al.*⁶⁵ developed a hydrogel driven by dynamic Schiff base bonds made from gelatin and OSA, which effectively responds to an acidic infectious microenvironment, exhibiting notable tissue adhesion. They highlighted the

Table 2. Functionalization (chemical modification) and application of sodium alginate-based hydrogel

Sodium alginate content	Other main components	Reaction	Functionalization	Advantages	Applications	References
8 wt%	Chitosan, polyacrylamide, hydroxyapatite	Schiff base reaction	Graft polymerization	Self-healing, biocompatibility	Bone repair	61
30 wv%	Ethylenediamine gelatin	Schiff base reaction	Graft polymerization	pH response, antibacterial activity (<i>Escherichia coli</i> and <i>Staphylococcus aureus</i>), biocompatibility	Wound healing	65
25 mg/mL	Acrylamide, nanofibers, vancomycin	Photocross-linking	Graft polymerization	Adhesion (12.5 kPa), antibacterial (<i>S. aureus</i> and <i>Pseudomonas aeruginosa</i>), hemolytic properties	Wound healing	66
3 wt%	Quaternized chitosan	Schiff base reaction	Oxidation	Printability, self-healing, biocompatibility, antibacterial properties (<i>E. coli</i> and <i>S. aureus</i>)	Wound healing	26
10 wt%	β -carboxyethyl acrylate, acrylamide, N, N-methylenebisacrylamide, potassium persulfate, kanamycin, acrylic acid	Free radical polymerization	Graft polymerization	Drug delivery (9-aminoacridine and kanamycin sulfate), antibacterial activity (<i>E. coli</i> , <i>S. aureus</i> , <i>P. aeruginosa</i> , and <i>Bacillus subtilis</i>), pH sensitivity, cell compatibility	Drug delivery	67
2 wt%	Gelatin, zinc chloride	Ionic cross-linking	Oxidation	swelling ability (1,600%), antibacterial (<i>E. coli</i> and <i>S. aureus</i>), biocompatibility, biodegradability, drug delivery (antagomir-204-3p)	Bone repair	68
2 wv%	Rhodamine B, sodium dihydrogen phosphate, calcium sulfate	Ionic cross-linking	Sulfation	Printability, biocompatibility, loaded cells (dental follicle stem cell-derived small extracellular vesicles)	Gingival tissue treatment	69
10 mg/mL	Polyvinyl alcohol, polyacrylamide, tannic acid, cellulose nanocrystals	Free radical polymerization	Graft polymerization	Sensing (gauge factor of 8.39), self-healing	Flexible electronics	70
2 wv%	Methacrylate alginate, phenylglycine	Free radical polymerization	Graft polymerization	Biocompatibility, printability, hemostatic properties	Wound healing	71
70 mg/mL	Polyvinyl alcohol, borax	Free radical polymerization	Graft polymerization	Stretching (950%), self-healing, high toughness (122.21 kJ/m ³), sensing (gauge factor of 8.39)	Flexible electronics	72
2 wt%	Acrylic acid, acrylamide, ammonium persulfate, silica, ferric chloride	Free radical polymerization	Graft polymerization	Stretching (Tensile strength 1.46 MPa), sensing	Flexible electronics	73
1 wv%	Gelatin, calcium chloride, glutaraldehyde	Free radical polymerization	Graft polymerization	Transparency, swelling, biocompatibility	Corneal tissue engineering	74
8 wt%	Sodium tetraborate, chitosan, gelatin	Schiff Base reaction	Graft polymerization	Mechanical strength (compressive strength 2.43 MPa), self-healing, injectability, protein delivery (bovine serum albumin)	Drug delivery	75
4 wt%	Amino-functionalized graphene oxide, acrylamide	Photocross-linking	Graft polymerization	Self-healing ability, printability	Biological ink	76
1 wt%	Polyethylene glycol dimethacrylate, acrylamide	Free radical polymerization	Graft polymerization	Swelling and adsorption properties	Adsorbent	77

Abbreviations: wt%: Weight percent; wv%: Weight per volume.

hydrogel's ability to switch adhesion properties in response to temperature changes, allowing painless removal under low-temperature compression. This characteristic positions the hydrogel as a promising candidate for skin-friendly wound dressings, minimizing the discomfort typically associated with conventional adhesives. Jiang *et al.*⁶¹ created a hydrogel, forming a dual network using CMC, OSA, and PAM, termed CMCS-OSA-PAM. Mimicking natural cartilage ECM, researchers combined dynamic Schiff base chemistry with free radical polymerization. Sodium periodate (NaIO_4) worked on the SA sugar chain, targeting the diol groups nestled within. This oxidation process breaks the carbon-carbon single bonds and converts the neighboring hydroxyl groups into aldehyde groups. This modification was critical in converting SA into OSA. The swift creation of CMCS-OSA-PAM and CMCS-OSA-PAM-HA hydrogels in a mere 2 min (**Figure 3D**) was achieved through the Schiff base reaction, which linked the amino groups of CMCS with the aldehyde groups of OSA, alongside the free radical polymerization process of acrylamide (AM). The dual-network hydrogel was fabricated in a single step, where the primary and secondary networks emerged simultaneously, supporting each other while maintaining structural integrity. This hydrogel shows significant promise for use in cartilage tissue engineering applications.

2.2.2. Sulfation method

The sulfation method mainly involves sulfating SA with sulfate compounds. Sulfating SA swaps out its hydroxyl groups for sulfate groups, as shown in **Figure 2**, and cuts down hydrogen bonds. The resulting SA sulfate can be a model molecule for sulfated glycosaminoglycans found in cartilage and nerve tissue. These glycosaminoglycans are key players in the ECM, where they are instrumental in controlling how cells multiply, move, and differentiate, largely through growth factors. Specifically, introducing sulfate groups significantly increases the negative charge density of the material, enhancing its affinity for positively charged heparin-binding growth factors, such as vascular endothelial growth factor and fibroblast growth factor, forming a "molecular sponge" effect. This property enables hydrogels to combine stably and release bioactive molecules slowly through electrostatic interaction, thus prolonging their action time.⁷⁹ The negative charge on SA sulfate enables it to effectively bind to heparin proteins due to its attraction to the positively charged amino groups.⁸⁰ Therefore, sulfated-modified SA-based hydrogel shows multiple breakthrough values in biomedicine, such as growth factor regulation advantages, anticoagulation and blood compatibility, and cell behavior regulation ability. Stauber *et al.*⁶² achieved *in situ* enzymatic cross-linking with tyrosinase by double modifying alginate with sulfate and tyramine groups (**Figure 3E**). Hydrogel fosters a biomimetic, biocompatible niche promoting encapsulated bovine and human chondrocyte proliferation and specialization. In addition, the hydrogel binds to tyrosine residues in ECM collagen through tyrosinase, showing strong adhesion to cartilage tissue. The covalent cross-linking with tyrosinase also gives the alginate sulfate hydrogel stability *in vivo* when implanted subcutaneously in mice, supports the deposition of cartilage matrix components,

provides an injectable, bionic, adhesive, and stable system, and has broad application prospects in cartilage regeneration.

2.2.3. Grafting polymerization method

Graft polymerization-modified SA-based hydrogel is a material that modifies the structure of natural SA molecules by chemical means. Its core feature is that it combines the natural advantages of SA with the functional improvement of artificial modification. Specifically, the hydroxyl (-OH) and carboxyl (-COOH) groups on the main chain of SA are grafted to introduce hydrophobic groups, polymer chains, or functional molecules, significantly expanding its application range. For example, hydrophobic modification (such as grafting long-chain alkyl or aryl groups) can form an amphiphilic structure of originally hydrophilic SA, which can self-assemble in water to create particles with diameters ranging from nanometers to micrometers. This modification retains the high water absorption of SA (water absorption rate can reach thousands of times its weight).⁸¹ In terms of mechanical properties, graft polymerization significantly enhanced the structural stability of the hydrogel. The unmodified alginate gel relied on the "egg box structure" of divalent cations such as Ca^{2+} . However, such physical cross-linking was susceptible to disintegration due to the influence of ion displacement. A covalently crosslinked network can be formed by grafting polymers such as AM, significantly increasing the compressive modulus.⁸² Another outstanding advantage of graft polymerization modification is its multi-function integration ability. By grafting cell adhesion peptide, the cell affinity of hydrogel is significantly improved.¹⁷ Therefore, SA-based hydrogels modified by graft polymerization have great potential applications in precision drug delivery, environmental remediation, and tissue engineering. Qiao *et al.*⁶³ effectively integrated dopamine into oxidized alginate by harnessing the synergistic interplay of Schiff base and hydrogen bonding mechanisms involving dopamine, OSA, and CMC. This innovative approach created a highly durable hydrogel, demonstrating remarkable tissue-adhesive properties, photothermal therapy properties, and antibacterial capabilities, making it suitable for wound healing applications (**Figure 3F**). This hydrogel not only harnesses the benefits of alginate but also provides impressive antibacterial activity (killing over 99% of *Staphylococcus aureus* within approximately 5 min of light exposure and eliminating all *Escherichia coli* in just 10 min), along with substantial adhesion strength (5 kPa) and antioxidant efficiency (with oxygen elimination activity exceeding 90% in optimal conditions).

3. Applications of SA-based hydrogel

The functions of SA-based hydrogels have diversified through the above functionalization methods, and their performance has been constantly enhanced. These hydrogels can be precisely tailored to achieve optimal mechanical properties, ensuring they meet the specific requirements of various applications. Their excellent biocompatibility makes them suitable for a wide range of biomedical applications, while their self-healing capabilities add an extra layer of functionality. The versatility of SA-based hydrogels is further highlighted by their responsiveness to environmental stimuli, exceptional

absorbency, and ease of shaping and molding. These characteristics collectively position them as a multipurpose material suitable for biomedical engineering, environmental science, food science, and other research and application fields (Tables 1 and 2). Below is a detailed analysis of its applications in flexible electronics, tissue engineering, water treatment, food packaging, and wet electric generators.

3.1. Rehabilitation detection (Flexible electronics)

Accurate diagnostics, early detection systems, and rehabilitation tracking rely heavily on a dense network of sensors to deliver precise and timely evaluations.⁸³ Flexible sensors, known for their adaptability, sensitivity, and optical clarity, have become a focal point of cutting-edge research.⁸⁴ Among these, modified hydrogels are a prime candidate for crafting advanced biomedical flexible electronics due to their remarkable flexibility, porous structure, biocompatibility, and tissue-mimicking qualities. In practical applications, the strong adhesion and self-healing ability of hydrogels can ensure stable electrical signal transmission and improve the durability of sensors. To enhance the adhesion and self-fixing properties of hydrogels, researchers have been exploring various physical interactions, such as ionic bonds, metal coordination bonds, and hydrogen bonds.⁸⁵ In addition, double-network hydrogels, formed by two interwoven polymer networks, offer enhanced mechanical strength and fatigue resistance by fine-tuning intermolecular or intramolecular interactions. This breakthrough enables the creation of adaptable, multi-purpose flexible electronics.²

SA-based hydrogels are emerging as a promising material in flexible electronics, offering a range of significant advantages. To begin with, SA exhibits excellent biocompatibility, making it highly suitable for biomedical and tissue engineering applications. This is particularly crucial for flexible electronic devices that come into direct contact with the human body. In addition, SA can form hydrogels with various ions, resulting in materials with high ionic conductivity,⁸⁶ a property that significantly enhances the electrical performance of flexible electronic systems. Moreover, SA-based hydrogels possess remarkable mechanical properties, including flexibility and resilience, which enable devices to withstand repeated stretching and bending while maintaining optimal performance.⁸⁷ These hydrogels can also be chemically modified or combined with other materials to introduce advanced features such as antibacterial activity or self-healing capabilities, thereby broadening the potential applications of flexible electronics. Furthermore, SA is highly compatible with conductive substances such as carbon nanotubes and metallic nanoparticles.⁸⁸ When integrated, these components create a robust conductive network while preserving the hydrogel's flexibility, making it an excellent choice for developing cutting-edge flexible electronic devices.⁵⁰

Zhang *et al.*²³ developed a urea-SA composite hydrogel modified by urea. This innovative material serves a dual purpose: it functions as a wearable strain sensor and acts as an electrolyte in flexible zinc-ion batteries (ZIBs). Their findings suggest that the electrophysiological biomedical devices created from

this hydrogel hold promise for applications in personalized medicine. As depicted in **Figure 4A**, the system boasts a modular design with a network of interconnected circuits – energy, sensing, control, and display modules. The energy module, powered by three ZIBs wired in series, provides the necessary power to run the wearable sensor network. Before assembling the components, the researchers tested the self-sustaining, screen-printed flat batteries, putting them through their paces with constant charge-discharge cycles. These series-connected energy modules were capable of charging up to 5.4 V, demonstrating their ability to power the system reliably and confirming the effectiveness of the energy storage solution.

Zhuo *et al.*²⁴ created an interactive underwater human-machine interface by integrating the SA-based hydrogel sensor with the industrial manipulator, demonstrating the reliable electromechanical performance of the hydrogel sensor. The system operates through four distinct functional stages, illustrated in **Figure 4B**, including (i) the integrated gloves, equipped with five hydrogel sensor units, detect various hand movements through strain sensing, (ii) analog signals are converted into digital format and the data are analyzed, (iii) once the data are crunched, it is fed to the robotic arm's control panel, which kicks off the appropriate series of movements, and (iv) pneumatics handle the opening and closing of the gripper in real-time, allowing for the manipulation of objects underwater. Research indicates that this system allows users to put on integrated gloves and effectively control the movements of industrial robots in real-time, enabling precise and reliable operation of the robotic gripper for the swift retrieval of underwater items (**Figure 4B**). The system exhibits consistent performance and exceptional robustness.

When capturing brain signals, event-related potentials (ERP) are reliable for evaluating the effectiveness of non-invasive brain-computer interface (BCI) electrodes. By analyzing electroencephalogram (EEG) signals, ERP serves as a powerful tool for assessing brain activity. Xue *et al.*⁸⁹ developed an SA-based hydrogel and tested it alongside traditional wet and dry electrodes in a soundproof environment. Human volunteers participated in N170 BCI experiments using these electrodes, with the results illustrated in **Figure 4C**. The hydrogel and wet electrodes produced raw signals that were nearly identical, whereas the dry electrode significantly exhibited more noise. Both the wet and hydrogel electrodes demonstrated the anticipated negative peak around 170 ms, confirming the successful detection of ERP. Moreover, the EEG waveforms captured by the hydrogel electrode closely mirrored those of the wet electrode, with a peak time difference of <13 ms. In contrast, the dry electrode's waveform deviated noticeably from the other two, lacking a distinct negative peak within the N170 time window (**Figure 4C**). Notably, the hydrogel electrode outperformed the wet electrode in terms of longevity, maintaining consistent ERP detection for up to 12 h, compared to the wet electrode's 4-h functional limit. These findings highlight the practicality of the double-layer hydrogel electrode, which simplifies operation and enables prolonged, high-quality EEG recording. This innovation holds

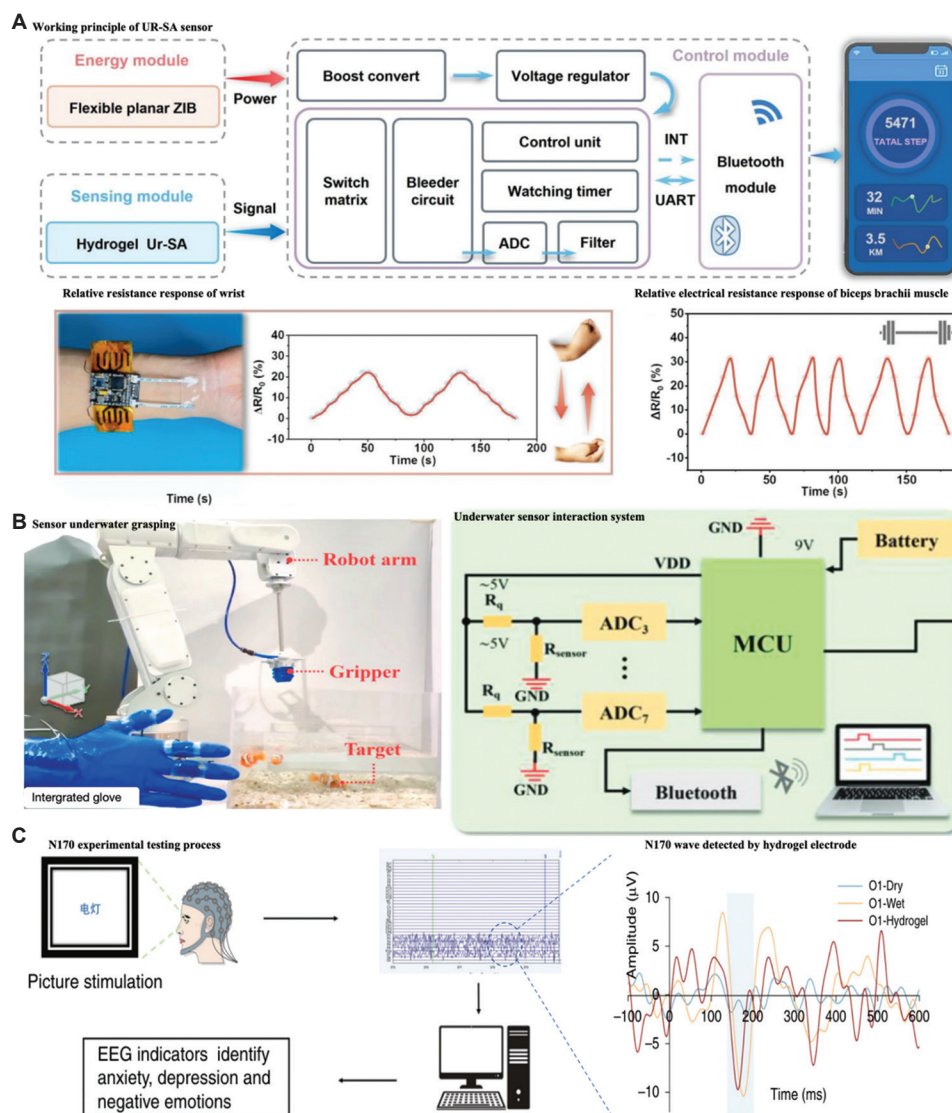


Figure 4. Flexible detection applications of sodium alginate-based hydrogels. (A) Working principle of the urea-modified sodium alginate (Ur-SA) sensor (top), relative resistance response for monitoring wrist and biceps curl movements (bottom).²³ (B) Image of the robotic arm gripper grasping underwater objects (left), underwater interactive human-machine interface system (right).²⁴ (C) Flow chart of event-related potential test experiment of double-layer hydrogel electrode (left), brain wave using dry, wet, and double-layer hydrogel electrode (right).⁸⁹ (A) Image used with permission from Royal Society of Chemistry, Copyright © 2024, Royal Society of Chemistry.²³ (B) Image used with permission from Wiley-VCH GmbH, Copyright © 2023, Wiley-VCH GmbH.²⁴ (C) Image used with permission from Springer Nature, Copyright © 2023, Springer Nature.⁸⁹

Abbreviations: ADC: Analog-to-digital converter; EEG: Electroencephalogram; GND: Ground; INT: Input; MCU: Microcontroller unit; UART: Universal asynchronous receiver transmitter; VDD: Drain voltage; ZIBs: Zinc-ion batteries.

significant promise for extending non-invasive BCIs into various everyday applications.

SA-based hydrogels often exhibit instability at extreme temperatures. Consequently, designing wearable strain sensors with high sensitivity, a broad sensing range, and environmental stability has emerged as a prominent research focus within flexible electronics and artificial intelligence. Zhang *et al.*⁹⁰ successfully fabricated a nanocomposite organic hydrogel utilizing ionic conductive PAM/SA and innovatively anchored a conductive coating of carbon nanotubes featuring an “island-bridge” microstructure. This hydrogel can be directly employed as an exceptional wearable strain sensor. It can achieve a sensing effect across a strain range of 0.1% to 600%, with a sensitivity

that can soar up to 76.54. Moreover, thanks to the incorporation of glycerol, these hydrogels can also accurately detect complex human activities within an ambient temperature range of 30°C – 50°C. This advancement paves a unique pathway for developing the next generation of wearable, flexible sensors, thereby holding substantial research significance.

This flexible electronic sensor, constructed using SA-based hydrogels, demonstrates exceptional mechanical performance and conductivity. This advancement opens up exciting possibilities for the next generation of wearable tech, including durable, self-healing, and adhesive devices. It holds significant potential for applications in flexible strain sensors and advanced electronic skin for health monitoring.

Various manufacturing techniques are involved in crafting flexible electronic devices from hydrogels. Bioprinting's precision in cellular organization, complex 3D construct fabrication, and efficient scalability render it a notable technique.⁹¹ Common techniques for molding SA-based hydrogels include extrusion,⁹² ink-jet printing,⁹³ and ultraviolet rays curing.⁹⁴ For successful printing, the SA-infused ink must be printable, and the choice of printing method dictates the type of ink required, which in turn influences the mechanical and biological properties of the final product.⁹⁵ Li *et al.*⁹⁶ used PVA, SA, cellulose nanofibers, and high-quality sodium borate tetrahydrate to develop a new type of composite hydrogel. This composite was remarkable; it demonstrates self-healing properties within half a minute, impressive electrical conductivity, and remarkable mechanical durability. This hydrogel can instantly self-heal, withstand a stress of up to 33.92 kPa, a tensile strain of up to 4,000%, and conduct electricity with a solid of 0.62 S/cm. Rheological tests revealed that at low strain frequencies, the loss modulus (G'') dominates the storage modulus (G'). However, as the strain increases, G' overtakes G'' , indicating a transition from sol to gel. This behavior is attributed to the hydrogel's hydrogen bonds, which initially resist strain but break under increasing pressure, causing a sharp drop in G' and a morphological shift. This sol-gel transformation makes it ideal for personalized 3D printing. Moreover, the hydrogel's viscosity decreases as the shear rate increases, allowing it to flow smoothly through a syringe and nozzle under pressure, making it well-suited for 3D printing. Its excellent rheological properties, self-healing characteristics, conductivity, and mechanical strength make it a standout material. Due to its excellent adaptability and high efficiency, bioprinting hydrogels have shown great advantages in the application of personalized wearable devices and physiological monitoring. However, their relatively low conductivity and tendency to absorb water in humid environments can compromise stability and reliability, limiting their applications. These issues need addressing in future research. In addition, using hydrogels as a support layer for suspension printing is an emerging technique that warrants further exploration.^{97,98}

3.2. Tissue engineering

Tissue engineering, a cutting-edge field at the intersection of cellular biology and materials science, focuses on creating tissues or organs in laboratory settings and within living organisms.²⁵ Hydrogels' 3D network architecture closely mimics the natural ECM, making them ideal scaffolds for fostering cell adhesion, growth, and specialization. Beyond their structural role, hydrogels serve as effective delivery systems for bioactive molecules, such as cytokines and growth factors, enabling controlled release to modulate the immune environment, maintain tissue balance, and stimulate cellular regeneration. These versatile properties position hydrogels as a promising biomaterial in tissue engineering.⁹⁹ Among these, SA stands out due to its low toxicity and rapid gelation, making it a popular choice.

3.2.1. Wound healing

Conventional wound healing therapies are grappling with the hurdles of tissue regeneration and functional restoration,

making hydrogels a highly promising alternative due to their distinctive benefits. As illustrated in **Figure 5A**, Yuan *et al.*¹⁰⁰ pioneered a novel strategy for tackling lower limb ischemia using a bioactive bioceramic composite hydrogel. They created a strontium/silicon-doped hydrogel that proved surprisingly effective in the early stages of ischemia. The *in vivo* study showed that this composite hydrogel, packed with strontium carbonate and calcium metasilicate, effectively protected muscle tissue in ischemic limbs from necrosis. Moreover, it promoted the growth of collateral capillaries, restoring blood flow to the affected area. The therapeutic success of this hydrogel is attributed to its controlled release of bioactive Sr^{2+} and SiO_3^{2-} ions, which work synergistically to facilitate angiogenesis, prevent muscle necrosis, and modulate physiological processes. These ions stimulate the production of key muscle regulatory factors (MyoG and MyoD) and vascular growth factors (vascular endothelial growth factor and hypoxia-inducible factor (1) while also providing direct protection to the vulnerable muscle tissue and encouraging the regeneration of capillaries. In addition, the hydrogel enhances M2 macrophage polarization whereas reducing M1 polarization, indirectly protecting muscle tissue and promoting blood vessel formation. The findings underscore that this bioactive hydrogel, rooted in inorganic bioceramics, offers a viable solution for treating lower limb ischemic diseases. Moreover, the design of such bioactive materials may pave the way for novel therapies targeting other ischemic tissue injuries.

Trauma-induced tissue damage has emerged as a significant concern in clinical settings, jeopardizing public health and safety. Conventional single-purpose wound dressings often fail to meet the multifaceted demands of effective wound healing. At the same time, the development and acquisition of multifunctional alternatives present significant challenges. To address this gap, SA has been chemically modified to augment its properties, positioning it as a highly promising solution for advanced wound care. Zhang *et al.*⁶⁶ introduced an innovative SA-based hydrogel dressing fabricated via a photocross-linking technique, which exhibits exceptional efficacy in accelerating wound recovery. This hydrogel can be rapidly customized on-site to conform to irregular wound shapes, providing unparalleled convenience. By meticulously adjusting the ratios of SA and AM, the hydrogel's structure and physicochemical properties can be precisely tailored to optimize performance. Research findings indicate that this composite hydrogel is a strong candidate for multifunctional wound dressing applications. *In vitro* studies on drug release and antibacterial activity have demonstrated its potent effectiveness against pathogens such as *S. aureus* and *Pseudomonas aeruginosa*. After just 4 h of incubation, the OD_{600} values for bacterial cultures were below 0.1, compared to 0.5 in the control group, highlighting its superior antimicrobial capabilities. Furthermore, coagulation activation tests, whole blood agglutination assays, and blood cell and platelet adhesion evaluations have confirmed the hydrogel's exceptional hemostatic capabilities, reinforcing its potential as a transformative wound care material. These findings underscore the immense potential of SA-based hydrogel as a versatile, high-performance medical dressing for wound healing. In addition to its complex pathophysiology,

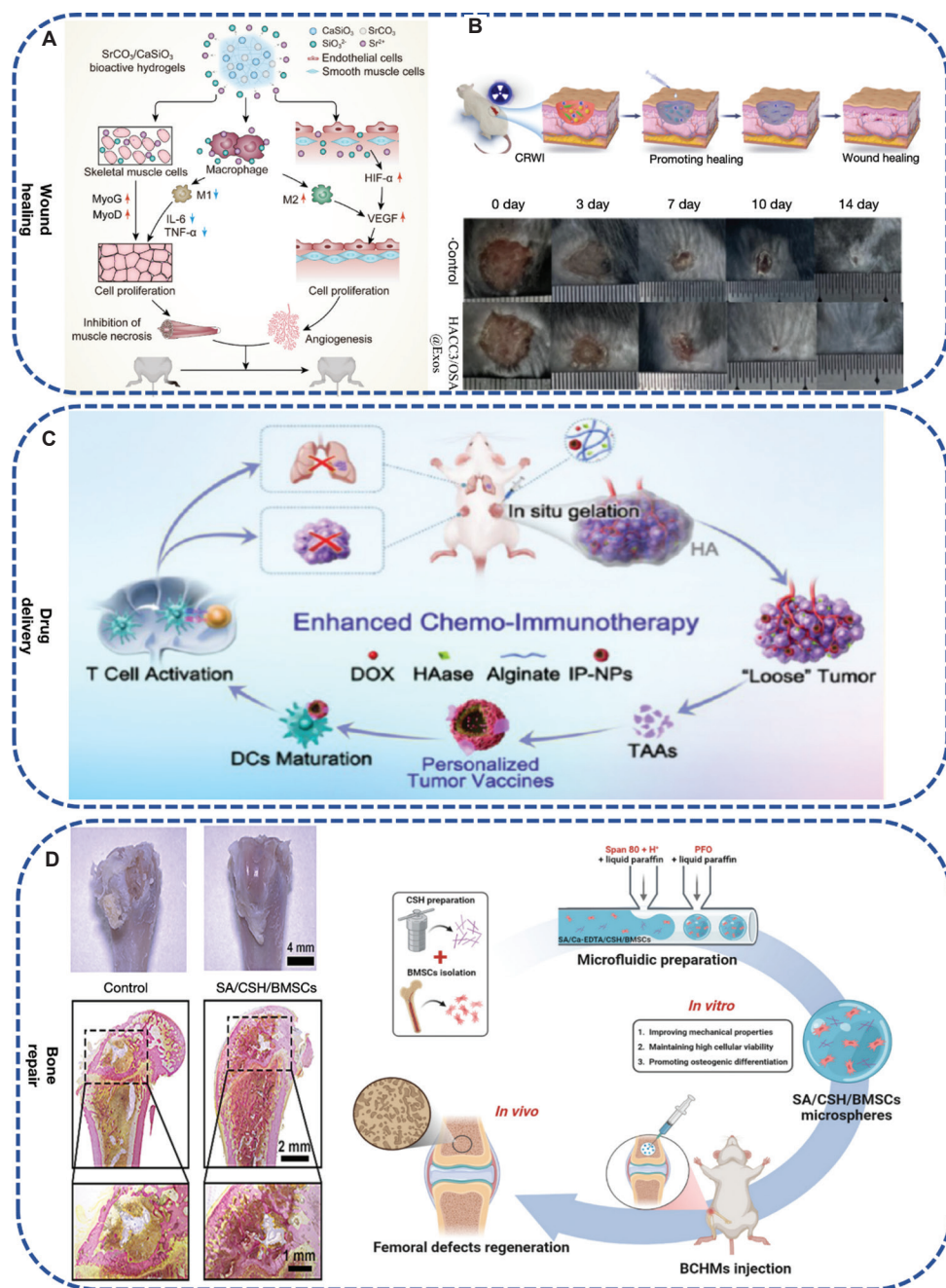


Figure 5. Tissue engineering applications of sodium alginate-based hydrogels. (A and B) wound healing applications of sodium alginate-based hydrogels. (A) Mechanism of Sr/Si-containing bioceramic/alginate composite hydrogel in the treatment of hind limb ischemia.¹⁰⁰ (B) Schematic diagram of a mouse wound injury and wound healing rate of the HACC/OSA hydrogel.²⁶ (C) Drug delivery applications of sodium alginate-based hydrogels. Injectable IP-NPs@ALG-DH were used to promote the penetration of DOX and the delivery of personalized tumor vaccines.²⁷ (D) Bone repair applications of SA-based hydrogels. SA/CSH/BMSCs hydrogel used in bone repair (left), repair mechanism (right).²⁸ (A) Image used with permission from Elsevier B.V., Copyright © 2023, Elsevier B.V.¹⁰⁰ (B) Image used with permission from Elsevier B.V., Copyright © 2024, Elsevier B.V.²⁶ (C) Image used with permission from American Chemical Society, Copyright © 2024, American Chemical Society.²⁷ (D) Image used with permission from Elsevier Ltd, Copyright © 2024, Elsevier Ltd.²⁸ Abbreviations: ALG: Sodium alginate; BCHM: Bioactive sodium alginate composite hydrogel microsphere; BMSCs: Bone marrow-derived stem cells; CSH: Xonotlite; DCs: Dendritic cells; DOX: Doxorubicin; HA: Hyaluronic acid; Haase: Hyaluronidase; HACC: Quaternized chitosan; HIF-1 α : Hypoxia-inducible factor 1-alpha; IL-6: Interleukin 6; IP-NPs: Micelles; Myo: Myosin; OSA: Oxidized sodium alginate; TAAs: Tumor-associated antigens; TNF- α : Tumor necrosis factor alpha; VEGF: Vascular endothelial growth factor; VG: Van Gieson.

diabetes wound is one of the most challenging health problems in the medical field today. Wang *et al.*¹⁰¹ prepared a pH/glucose dual bio-responsive color hydrogel particle, which is composed of hyaluronic acid methacryloyl alginate sodium anti-opal scaffold, filled with dextran oxide/quaternized CS

and loaded with glucose oxidase, antimicrobial peptide, and vascular endothelial growth factor. Due to the high glucose environment of diabetes wounds, glucose oxidase will catalyze the production of acidic products from glucose, leading to pH changes, and antimicrobial peptide and vascular endothelial

growth factor will be released rapidly. This is a controllable process, accompanied by changes in particle structure and color, which provides great help for wound detection. Therefore, this type of hydrogel particle with the dual response of pH/structural color shows great advantages in diabetes wound treatment.

Catheter-related wound infections (CRWIs) present unique challenges compared to standard injuries. They complicate the healing process due to the onset of severe inflammation, tissue necrosis, and disruption in the formation of new blood vessels. Conventional wound care approaches are often insufficient in addressing these complex issues. Peng *et al.*²⁶ developed an innovative polysaccharide-based hydrogel infused with exosomes, demonstrating remarkable promise in speeding up CRWI recovery. This hydrogel possessed consistent rheological characteristics, ensuring a steady release of exosomes from mesenchymal stem cells (MSCs), which fosters tissue repair. With its bioadhesive and self-healing capabilities, the hydrogel dressing shields CRWI from external environmental stressors, offering a robust and sustained antibacterial defense. By delivering exosomes at the right time, the hydrogel stimulates blood vessel growth, boosts cell proliferation, encourages granulation tissue formation, and aids collagen buildup, making it a powerful tool for skin regeneration post-CRWI. A CRWI model was created in mice following whole-body irradiation (**Figure 5B**), which exhibited symptoms consistent with acute radiation exposure to test its efficacy. Compared to the control group, untreated CRWI mice experienced a notable slowdown in wound healing ($p < 0.001$), confirming the model's validity. The healing trajectory revealed that the exosome-loaded hydrogel outperformed other treatments, emerging as the most effective solution for radiation-induced wounds. As a result, this hydrogel stands out as a cutting-edge wound dressing, capable of promoting tissue regeneration, providing healing support, and delivering long-lasting antibacterial protection in the aftermath of CRWI.

Unlike traditional two-dimensional cell cultures, 3D models offer a more accurate representation of the *in vivo* cellular microenvironment, enhancing the diffusion of nutrients and oxygen. While many tissue engineering scaffolds are made from synthetic polymers, these often rely on toxic biological cross-linking agents to achieve mechanical strength.¹⁰² Hydrogels, which consist of hydrophilic polymer chains forming 3D molecular networks, have gained widespread use as scaffold materials in this field. SA, in particular, has emerged as a key ingredient for creating hydrogels in tissue engineering and drug delivery, thanks to its biocompatibility and ease of gelation¹⁹. These 3D scaffolds are pivotal in advancing tissue regeneration and repair. Moreover, 3D enables the creation of structures that closely resemble human tissue, providing a more accurate representation of the biological environment. This advancement holds great potential for facilitating transplantation studies in the future.¹⁰³ 3D printing, coupled with SA-based hydrogels, expands tissue engineering possibilities.¹⁰⁴

Jiao *et al.*¹⁰⁵ delved into how collagen/SA-based hydrogels, formulated in different ratios, swell, degrade, and behave

under a microscope. They also checked their compatibility with living tissue, intending to use them in skin bioprinting. They found that higher SA concentrations enhanced the hydrogel's mechanical strength and swelling capacity while accelerating its degradation rate. In addition, these hydrogels exhibited smaller pore sizes and superior biological compatibility. Among the tested formulations, the 1% collagen hydrogel stood out, demonstrating enhanced fibroblast and keratinocyte spreading and proliferation when used to print a dual-layer skin structure. The study concluded that collagen/SA-based hydrogels possess excellent printability, making them a promising bioink for skin bioprinting. This breakthrough paves the way for advancing 3D modeling in wound healing research.

3.2.2. Drug delivery

The porosity of hydrogels is crucial for the transport of various bioactive compounds, including drugs, genes, and peptides or proteins.¹⁰⁶ Consequently, hydrogels formulated with SA are often employed for effective drug delivery.

El-Sayed *et al.*⁶⁷ introduced a novel drug delivery system, ingeniously crafted by grafting SA with carboxyethyl acrylate and AM. They incorporated 9-aminoacridine and kanamycin sulfate into the hydrogel matrix during the graft polymerization. The grafting efficiency of this cutting-edge hydrogel ranged from a solid 70.01% to an impressive 78.08%. They conducted thorough analysis to determine the hydrogel's chemical structure, thermal stability, and physical characteristics. Interestingly, swelling tests showed that the plain, drug-free gel swelled up more than the drug-packed one. In addition, antibacterial assessments indicated that the hydrogels loaded with either 9-aminoacridine (88.6%) or kanamycin sulfate (89.3%) demonstrated commendable antibacterial properties against Gram-positive and Gram-negative bacteria. The inhibition zones observed for *E. coli*, *P. aeruginosa*, *Bacillus subtilis*, and *S. aureus* were 17 mm, 14 mm, 19 mm, and 21 mm, respectively. Finally, a cytocompatibility evaluation using normal lung cell lines indicated that the drug-loaded gel posed minimal toxicity. In contrast, the blank hydrogel achieved a cell survival rate of 92.5%, thus confirming its viability for biomedical applications.

Furthermore, the limited ability of chemotherapy agents to effectively penetrate tumors and create viable tumor vaccines within the body significantly hampers the efficacy of chemotherapy and immunotherapy. To tackle this issue, Yang *et al.*²⁷ engineered an innovative injectable SA system designed to boost the effectiveness and depth of doxorubicin (DOX) delivery in chemotherapy, while also streamlining the process of administering tailored tumor vaccines. As illustrated in **Figure 5C**, this innovative SA platform rapidly forms hydrogels upon exposure to physiological levels of Ca^{2+} , allowing it to act as a reservoir for drugs that gradually and consistently release hyaluronidase, DOX, and micelles. Hyaluronidase targets the excessively produced hyaluronic acid within tumor tissues, effectively loosening the structure and enabling deeper infiltration of the remaining components. Meanwhile, DOX can trigger robust immunogenic cell death and generate tumor-associated antigens efficiently captured

by polyethyleneimine-coated micelles to create personalized tumor vaccines. These vaccines are instrumental in promoting dendritic cell maturation and T lymphocyte activation, ultimately establishing long-lasting immune memory. In addition, the released drugs bolster the immune response, inciting a more potent anti-tumor effect. Studies indicate that this drug delivery system demonstrates remarkable effectiveness in treating colorectal cancer.

The delivery of stem cells is a focal point in medical research. Shear forces and fluid tension can stress and damage the stem cell membrane, leading to low survival rates. Xiang *et al.*¹⁰⁷ proposed a protective strategy: encapsulating piezoelectric barium titanate nanoparticles in an Arg-Gly-Asp (RGD)-OSA and hyaluronate amine hydrogel. These nanoparticles boost intracellular free Ca²⁺ levels via electrical stimulation, offering immediate cell protection. The RGD-OSA/hyaluronate amine hydrogels reduce injection-induced membrane damage with tunable mechanical properties and shear-thinning behavior. This approach significantly enhances stem cell survival rates, prolongs *in vivo* retention time, and boosts tissue repair efficacy, showing great potential for cell therapy and tissue regeneration.

Meanwhile, Long *et al.*¹⁰⁸ proposed a method for treating colorectal cancer using near-infrared (NIR) photothermal therapy combined with chemotherapy drug delivery. They developed an injectable butynamide-SA-MoS₂-5-fluorouracil adhesive hydrogel. MoS₂ nanosheets, with their excellent dispersion and NIR-triggered photothermal effect, can directly induce cancer cell degeneration and damage through hyperthermia. Simultaneously, the hydrogel delivers the chemotherapy drug 5-fluorouracil, showing a strong therapeutic effect in inhibiting cancer cell proliferation and promoting colorectal tumor regression. This strategy of combining hyperthermia with chemotherapy offers a promising approach for the local treatment of colorectal cancer and holds significant potential.

Although studies have illuminated the promise of SA-based hydrogels in drug delivery applications, their real-world implementation faces a significant roadblock: Their restricted loading capacity limits their capabilities in handling a wider spectrum of medications. Moreover, although SA itself boasts excellent biocompatibility, the safety and cellular effects of its derivatives or chemically altered forms remain understudied. Future progress in functionalization methods is vital for maximizing hydrogel efficacy in pharmaceutical delivery.

3.2.3. Bone repair

Bone regeneration via hydrogels presently faces key obstacles. Conventional hydrogels, typically soft and pliable, often fall short of delivering the necessary mechanical support, limiting their effectiveness in this field. To address this, researchers have recently turned to blending SA with other materials through physical mixing and cross-linking techniques, resulting in hydrogels with enhanced mechanical properties. These advanced gels open possibilities for 3D-printed scaffolds, providing structural integrity and a prime environment for bone cell development and specialization. SA-based hydrogels,

with their easily adjustable thickness, are excellent bioinks. This allows us to 3D print custom-made scaffolds perfectly suited for fixing bone injuries.¹⁰⁹ In a notable study by Jiang *et al.*,⁶¹ they created a dual-phase hydrogel framework for osteochondral repair via Schiff base chemistry coupled with free radical polymerization. The hydrogel is formulated from a blend of CMC, OSA, and PAM, collectively called CMC-OSA-PAM. HA was integrated into the CMCS-OSA-PAM hydrogel to enhance the subchondral bone layer, resulting in the development of a CMC-OSA-PAM-HA hydrogel. The dynamic imine bonds within the hydrogel facilitated interlayer interpenetration, enhancing bonding strength through the hydrogel's continuous matrix and self-healing properties. *In vitro* studies demonstrated the hydrogel's excellent biocompatibility, highlighting its promising potential for osteochondral tissue engineering applications.

Mesenchymal stem cells are a type of adult stem cell with self-renewal and multipotent differentiation potential. They are widely distributed in various human body tissues and have shown significant value in regenerative medicine and immunotherapy. MSCs are widely distributed in multiple tissues of the human body. MSCs from different sources have certain differences in proliferation ability and function, as well as unique biological characteristics and strong regenerative ability.¹¹⁰ The advantage of using MSCs to induce differentiation of bone or cartilage-like organs is their ability to rapidly proliferate and differentiate into various mesenchymal-derived tissues. MSCs have broad application prospects in tissue engineering and regenerative medicine. They can differentiate into bone or cartilage cells and regulate the local microenvironment by secreting soluble factors and extracellular vesicles, thereby promoting tissue repair and regeneration.¹¹¹ Hydrogel delivery of MSCs is a cutting-edge technology combining biomaterials and stem cell therapy. It uses a 3D network structure of hydrogels to simulate the ECM, provide a suitable microenvironment for MSCs, and achieve efficient cell delivery and functional regulation.¹¹²

Jiang *et al.*²⁸ developed a novel system of bioactive SA composite hydrogel microspheres to address the challenges of irregular and lacunar bone defects. As illustrated in **Figure 5D**, the researchers incorporated xonotlite (CSH) nanowires to enhance the biological activity of the existing SA hydrogel microspheres. As an innovative delivery mechanism for stem cells, bioactive SA composite hydrogel microspheres successfully preserved the high activity levels of the encapsulated bone marrow-derived stem cells (BMSCs). The inclusion of CSH nanowires enhanced the SA microspheres' structural integrity. Interestingly, adding 12.5% CSH to these microspheres increased osteogenic gene expression. This, in turn, promoted solid bone regeneration in a rat model with femoral defects. The control group in the figure clearly shows cartilage defects, which may be due to strong inflammatory reactions after surgery. In contrast, the group that received the composite SA microsphere treatment (SA/12.5%, CSH/BMSCs) showed a significant increment in bone regeneration. Specifically, in the SA/12.5% CSH/BMSCs group, the cartilage layer was back to normal, with the new cartilage tissue blending right in with the surrounding areas.

This research provides significant assistance in repairing these challenging porous bone defects.

However, SA has certain limitations when used for bone tissue regeneration, as it lacks inherent osteoconductivity and osteoinductivity, which are crucial for promoting bone growth and integration. While SA alone may not induce cell differentiation, introducing magnetic responsive nanoparticles into hydrogel scaffolds can achieve precise targeting of specific damage sites by injecting them after applying magnetic fields. Hia *et al.*¹¹³ used SA as a raw material, embedded with calcium phosphate-encapsulated superparamagnetic iron oxide nanoparticles, and prepared a new microsphere hydrogel. This gel microsphere exhibits magnetic targeting properties, enhances hydrogel cross-linking, controls degradation rates, and possesses strong antibacterial activity. Experimental results have shown that the viability and proliferation of encapsulated cells (MC3T3-E1) are significantly enhanced, with increased alkaline phosphatase activity and mineralization levels. In addition, collagen production within the microspheres is augmented. These hydrogel microspheres promote cell proliferation, osteogenic differentiation, and matrix mineralization, holding great promise as a multifunctional material for bone tissue repair.

Wu *et al.*²⁹ engineered an advanced multifunctional hydrogel system with smart responsiveness, integrating NIR-triggered mild photothermal therapy to precisely control macrophage polarization and vascular development, accelerating bone regeneration. The remarkable bone augmentation observed with the hydrogel platform stems from its versatile therapeutic capabilities, as illustrated in **Figure 5D**. First, the synergistic interaction of black phosphorus, polydopamine, and deferoxamine enables the hydrogel to sustain a regenerative-friendly microenvironment throughout the repair process, due to its potent osteogenic and angiogenic properties vital for healing bone defects. Second, when exposed to mild NIR irradiation, the hydrogel effectively shifts macrophage polarization toward the M2 phenotype, boosting the production of anti-inflammatory, angiogenic, and osteogenic cytokines. This innovative approach significantly enhances the recruitment of new blood vessels and endogenous stem cells, which are crucial in the initial stages of the healing process. In addition, black phosphorus nanosheets, a key hydrogel component, endow the material with mild photothermal activity, pH sensitivity, and NIR-triggered drug/ion release capabilities. These features ensure efficient bone regeneration by providing targeted and controlled therapeutic interventions. Moreover, the long-term integration of physical (mild thermal therapy) and chemical (drug/ion delivery) interventions creates an intelligent, responsive treatment system. This system optimizes the regenerative microenvironment and promotes effective bone repair by synergistically combining multiple therapeutic modalities. Overall, the NIR-activated hydrogel emerges as a highly promising biomaterial scaffold. It can address large bone defects by fostering M2 macrophage accumulation, reducing inflammation, stimulating angiogenesis, and enhancing bone matrix deposition. This multifunctional hydrogel significantly advances bone tissue

engineering and regenerative medicine. The study successfully demonstrated its efficacy using a critical-size skull defect model, where the hydrogel group exhibited significantly greater new bone formation at 4 weeks and a complete bone structure by 8 weeks compared to controls. By merging intelligent, responsive design with bioactive factors, the research offered an innovative and impactful strategy for bone regeneration, highlighting the hydrogel's vast potential in bone defect repair applications.

3.3. Other applications

In addition to flexible electronics and tissue engineering, SA-based hydrogels have unique applications in water treatment, food, and wet electric generators.

3.3.1. Water treatment

Hydrogels have garnered significant attention in environmental applications, such as wastewater treatment, due to their exceptional water-swelling capacity and inherent hydrophilicity, primarily attributed to their ionic nature. These characteristics render them highly effective as adsorption materials.¹¹⁴ Their high specific surface area, superior pore connectivity, and overall efficiency significantly enhance their adsorption capacity and speed. These materials are distinguished by their rapid swelling kinetics, customizable surface properties, extensive surface area, tunable pore structure, permeability, and pH sensitivity, which collectively broaden their utility in wastewater treatment applications. Among bio-based adsorbents, SA stands out as a particularly promising option.¹¹⁵ Its high hydrophilicity, biodegradability, and cross-linking ease make it a versatile candidate for various applications. Through physical and chemical modifications, SA can be tailored to introduce additional functional groups, boosting its adsorption efficiency, mechanical strength, and durability.¹¹⁶ Moreover, its biological safety, biocompatibility, and renewability position it as a highly promising material for sustainable wastewater treatment solutions. The molecular structure of SA, rich in carboxyl and hydroxyl groups, grants it a strong affinity for various pollutants. These functional groups can also engage in specific interactions with contaminants, enabling selective removal.¹¹⁷ Modified SA further enhances its performance by increasing its surface area, porosity, and active sites.¹¹⁸ Using modified SA-based hydrogels in water treatment is an area of ongoing research and innovation, with significant potential for future advancements.

Berg *et al.*¹¹⁹ meticulously documented the development of a polyethyleneimine-enhanced alginate hydrogel, scrutinizing its swelling and degradation behavior across a spectrum of aqueous and organic environments under diverse conditions. Their comprehensive study unveiled the composite hydrogel's capacity for selective and precise adsorption within a model dye system. Notably, the alginate hydrogel demonstrated an adsorption rate of methylene blue at 2.31×10^{-4} mol/g, whereas the polyethyleneimine-alginate composite hydrogel exhibited an adsorption rate of Congo red at 6.69×10^{-5} mol/g. Further exploration of the pH-dependent adsorption characteristics highlighted the material's robust performance across various acidic and alkaline conditions. These findings underscore

the significant potential of the polyethyleneimine-alginate composite as a viable and effective solution for future wastewater treatment applications.

Yu *et al.*³⁰ ingeniously integrated the advantageous properties of hydrogels and fabrics to create a hydrogel fiber fabric (HHF-C) evaporator. Through optimization of the HHF-C evaporator's structure (**Figure 6A**), they achieved efficient water transport, localized heat retention, and reduced water evaporation enthalpy. Consequently, the HHF-C evaporator exhibited an impressive evaporation rate of 4.13 kg·m²/h when tested in a simulated saline environment with a 20 wt% salt solution. According to statistics, most evaporators on the market have an evaporation rate of only about 2 kg·m²/h, and the comprehensive performance of HHF-C evaporators is better than the research before this study. The evaporator's surface remained free of salt deposits even after 8 h of sunlight exposure, setting a new benchmark in the field. The team validated the water transport and heat localization mechanisms through experimental and numerical simulations, with the findings aligning closely and confirming the soundness of their approach. Furthermore, they successfully fabricated large-scale HHF-C evaporators measuring 13 × 100 cm² and 20 × 20 cm², demonstrating their practicality for real-world seawater desalination applications. As illustrated in **Figure 6A**, the evaporator was tested outdoors under natural sunlight, where a transparent acrylic model house with a sloped roof facilitated sunlight penetration and heated the HHF-C evaporator. The sloped design also aided in collecting the condensed freshwater. Water quality was assessed using inductively coupled plasma optical emission spectroscopy, which measured the concentrations of key ions (Na⁺, K⁺, Ca²⁺, Mg²⁺) before and after desalination. The findings revealed that the ion concentrations in the treated water were significantly lower than the thresholds set by the World Health Organization. Moreover, the HHF-C evaporator effectively removed organic dyes such as rhodamine B and methylene orange from contaminated water. These results highlight the device's promise to scale up seawater desalination and purification efforts. The research also presents an innovative design framework that pushes the envelope in solar vapor generation systems, delivering impressive evaporation rates, robust salt resistance, and the potential for mass production.

3.3.2. Food packaging

Bio-based hydrogels are gaining significant traction in the food packaging industry, driven by their unique advantages. However, their widespread adoption in the food sector is still somewhat limited. Recently, there has been a surge of interest in harnessing advanced bio-based hydrogel technologies to reduce the dependence on non-biodegradable synthetic plastics derived from fossil fuels. Certain hydrophilic polymers exhibit the remarkable ability to swell in water, absorbing volumes many times their own weight, ultimately forming 3D crosslinked hydrogels.¹²⁰ Given their accessibility, biodegradability, and biocompatibility, these hydrogel films show great potential for revolutionizing the food packaging industry. Take SA-based hydrogels, for instance; they're non-toxic, biocompatible, and excellent at forming films, making them a natural fit for food packaging. However, on their own,

SA-based hydrogels fall short in terms of mechanical strength and functional versatility. To address this, blending them with other materials becomes essential to boost their mechanical and functional properties, paving the way for their effective use in food packaging.¹²¹

Yang *et al.*¹²² crafted nanocellulose hydrogels with boosted tensile characteristics, fatigue resistance, high water-holding capacity, and antibacterial traits. They utilized soybean shell nanocellulose, PVA, SA, and TA. When heated, TA comes with catechin groups that undergo *in situ* polymerization, creating polymers with a larger molecular weight. Due to intermolecular interactions, various raw materials form tight crosslinks, making the solution thicker. The hydrogel's ester bond breaks as pH increases, enhancing its swelling and release properties. Mechanical tests show this hydrogel has excellent tensile properties, viscoelasticity, and mechanical strength (compressive strength is 10 kPa, tensile strength is 0.35 MPa). In weakly acidic and alkaline environments, as the pH increases, the ester bond of the hydrogel breaks, further improving its swelling and release behavior. The hydrogel's equilibrium swelling rate exceeded 300%, and the release rate of TA was over 80%. The hydrogel proved its mettle in antibacterial trials, successfully eliminating *S. aureus* and *E. coli* while also keeping refrigerated chicken fresh for up to 10 days. Due to these characteristics, it exhibits significant advantages in extending the shelf life of frozen meat products. With its budget-friendly production and simple preparation process, this hydrogel has the potential for diverse applications across the food sector.

Hadi *et al.*³¹ used SA and aloe vera as base materials and combined them with collagen (GT) and hydroxypropyl methylcellulose (HPMC) to improve the performance of the resulting composite film. A comprehensive comparative analysis was conducted to evaluate the effects of these additions on the film's physical and mechanical attributes. The results indicated that both GT and HPMC significantly augmented the tensile strength of the composite film. The tensile strength reached a maximum of 68.25 MPa at GT concentrations of 12% and HPMC concentrations of 52.19%. Moreover, incorporating these hydrogels into the polymer matrix improved the film's flexibility and increased its thickness, moisture content, swelling capacity, and water vapor permeability. However, the addition of GT had some drawbacks. It led to a substantial reduction in oxygen permeability, which decreased from 1.46 × 10⁻¹⁵ to 0.45 × 10⁻¹⁵ g/m/s/Pa at higher GT concentrations. In addition, the presence of GT caused a decline in the film's solubility, with a notable drop to 23.12% observed at a 14% GT concentration. Despite these challenges, the study highlights the significant positive impact of both GT and HPMC on the mechanical performance of alginate-aloe composite films, underscoring their potential for advanced applications in biocompatible and functional materials.

Yu *et al.*¹²³ developed a soy hull nanocellulose/SA/CaCl₂ composite hydrogel film with remarkable mechanical strength, transparency, and conductivity. This was achieved by freezing at -80°C, cross-linking through hydrogen and ester bonds, and ionic cross-linking. The researchers then evaluated the

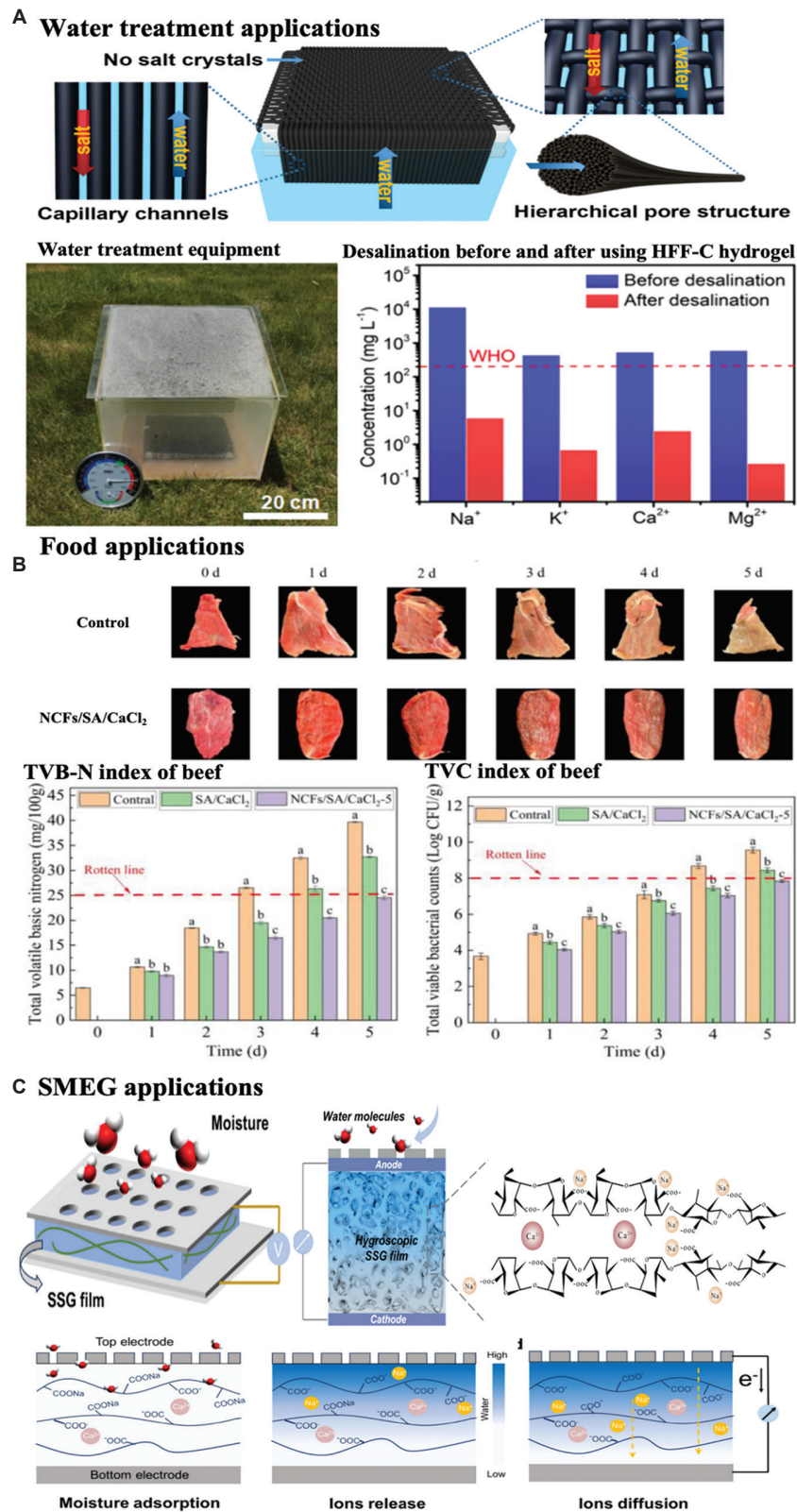


Figure 6. Environment, food, and electric generator applications of sodium alginate-based hydrogels. (A) HFF-C hydrogel evaporator.³⁰ (B) Food packaging application of NCFs/SA/CaCl₂ hydrogel.¹²³ (C) Electrical output mechanism and device diagram of SMEG prepared by SSG hydrogel.³² (A) Image used with permission from Elsevier Ltd, Copyright © 2023, Elsevier Ltd.³⁰ (B) Image used with permission from Elsevier Ltd, Copyright © 2024, Elsevier Ltd.¹²³ (C) Image used with permission from Elsevier Ltd, Copyright © 2024, Elsevier Ltd.³² Abbreviations: HFF-C: Hydrogel fiber fabric; NCFs: Nanocellulose; SMEG: Sodium alginate wet electric generator; SSG: SA-SiO₂-rGO; TVB-N: Total volatile basic nitrogen; TVC: Total viable bacterial counts, (SMEG); WHO: World Health Organization.

Advances in sodium alginate-based hydrogels

hydrogel film's impact on extending the shelf life of beef. When the meat was wrapped with the composite hydrogel film, it absorbed moisture from the surface, allowing it to adhere and form a protective layer (**Figure 6B**). This layer could be easily removed without damaging the beef's tissue structure. Over a period of 0–5 days, the levels of volatile basic nitrogen and total viable bacterial count in the meat were monitored (**Figure 6B**). The findings revealed that the hydrogel extended the beef's preservation period, inhibited microbial growth, and maintained tissue integrity. Consequently, this hydrogel is an innovative packaging material that ensures the quality and safety of meat products at room temperature. The soy hull nanocellulose/SA/CaCl₂ composite hydrogels, known for their tensile strength, transparency, and high conductivity, hold significant promise for applications in smart food packaging and detection technologies.

3.3.3. Wet electric generator

Moisture-enabled energy generation (MEG) represents an innovative approach to harnessing environmental energy by converting atmospheric water vapor into electricity.¹²⁴ Given the omnipresence of water vapor and this process's eco-friendly, emission-free nature, MEG research holds substantial scientific and practical importance. Hydrogel-based hygroscopic materials, with their flexible 3D polymer networks, generally outperform carbon-based counterparts in moisture absorption.¹²⁵ However, current hydrogel-based MEGs have yet to deliver satisfactory current outputs. The efficiency of these generators relies on the directional movement of ions within the hydrogel. While ionic conductivity is a key factor influencing electrical performance, strong hydrogen bonds between polymer chains often impede the mobility of free charge carriers. This limitation reduces ionic conductivity in pure hydrogel materials, ultimately hampering their current output potential.

Huang *et al.*³² developed a cutting-edge power generation system that uses hydrogel matrix composites. These composites can absorb moisture and exhibit remarkable ionic conductivity, clocking in at 1.46 S/m. The SA wet electric generator (SMEG), which features a single SA-SiO₂-reduced graphene oxide (rGO) hydrogel film, shows top-notch efficiency. Under 40°C and 80% relative humidity conditions, it can generate an open-circuit voltage of about 0.6 V and a short-circuit current density of roughly 0.14 mA·cm². The improved power generation capabilities of the SMEG increase energy conversion efficiency and reduce the number of units required for power supply. The basic principle behind MEGs is the directional movement of ions spurred on by concentration gradients. When water comes into contact with the device, it causes hygroscopic substances to break apart, releasing a flood of mobile protons from hydrophilic groups such as hydroxyl and carboxyl. At the same time, negatively charged functional groups stay put, firmly attached to the structural framework of the absorbent material. The electrical signal generated by positively charged ions flowing along a concentration gradient can be detected in the external circuit. The self-powered microenergy generator developed leans into this mechanism, giving significant electrical performance (**Figure 6C**).

Essentially, the SMEG unit sandwiches the SA-SiO₂-rGO (SSG) film, which is the engine for power generation, between two electrodes that are not identical. Unlike the common MEGs that rely only on hydrophilic groups for water adsorption, adding the deliquescent salt CaCl₂ greatly enhances the moisture absorption capacity of the SSG membrane. Moreover, when the SA chain's numerous hydrophilic groups come into contact with water, they release many sodium ions. The Ca²⁺ in the SSG membrane breaks up the hydrogen bonds between polymer chains through the Hofmeister effect, widening the ion transport channels and increasing conductivity. These findings provide new ways of designing multifunctional materials with stable porous structures and high conductivity. Comparing the output performance of SMEG with previously reported MEGs in terms of open-circuit voltage and short-circuit current density, the output open-circuit voltage of most previously reported MEGs is <0.6 V, with a short-circuit current density of <10 μA cm⁻². This means these MEGs require an area >100 cm² to achieve an output current of 1 mA. In contrast, the current output of SMEG is 140 μA cm⁻², meaning that an SMEG with a size of 16 cm² can easily achieve an output current exceeding 1 mA. This lays a foundation for the development of MEG energy-saving devices.

4. Future perspectives

In summary, SA-based hydrogels have garnered significant attention across various fields, including flexible electronics, tissue engineering, food preservation, and water treatment. This widespread popularity is attributed to their tunable mechanical properties, biocompatibility, self-healing capabilities, adaptability, responsiveness to environmental stimuli, high absorbency, and ease of shaping. Despite these remarkable attributes, there remains substantial potential for further enhancement and innovation in developing and applying these hydrogels. Continued advancements can be achieved by focusing on several key areas, as depicted in **Figure 7**.

Regarding flexible electronics, SA-based hydrogels possess a degree of conductivity but generally fall short compared to metals or conductive polymers, limiting their application in flexible electronics requiring high conductivity. Specifically, the conductivity of SA-based hydrogels typically does not exceed 100 S/cm, which is insufficient to meet the requirements of digital circuits and bioelectronics applications. Building on the current research foundation, achieving the collaborative optimization of conductivity and mechanical strength in SA-based hydrogels can be approached through several strategic methods. First, we can prepare an integrated hydrogel that carefully selects materials to enhance conductivity and mechanical properties. For instance, rGO, derived from graphene oxide, offers conductivity and mechanical reinforcement. Alternatively, MXenes can synergistically crosslink with SA to enhance performance. Second, the dynamic double network system of hydrogels holds great potential. SA-Ca²⁺ ion cross-linking provides conductivity, while covalent cross-linking, such as thiol-ene click reactions, enhances mechanical properties. Dynamic bonds, such as

disulfide and imine bonds, can reconstruct conductive paths after fracture, thereby extending the operational life of the hydrogel. Finally, we can design layered structures through biomimetic approaches, such as mimicking nacre layers to achieve high strength and ionic conductivity through alternating stacks of SA and clay. Conductive fillers can also be precisely oriented and arranged using 3D printing to optimize conductivity and mechanical properties in specific directions. While promising in various biomedical applications, SA-based hydrogels present significant limitations in terms of stability and durability under specific environmental conditions. These hydrogels are particularly susceptible to degradation and structural alterations when exposed to elevated temperatures or extreme pH levels. Although certain alginate hydrogels demonstrate self-healing properties, these capabilities are often limited and typically necessitate specific conditions or prolonged durations to manifest. Such constraints are suboptimal for applications in flexible electronics, where rapid self-repair is essential. In high-humidity environments, introducing hydrophobic groups can modulate the hydrophilicity of SA-based materials. This can be achieved by grafting hydrophobic chain segments, such as alkyl chains or polycaprolactone, onto the SA molecular chains or compositing hydrophobic materials to reduce water affinity. Under extreme pH conditions, materials can form more stable coordination bonds through ion covalent synergy or multivalent metal ion cross-linking, ensuring stability across different pH environments. In addition, a built-in buffer system, such as encapsulated phosphate buffer microspheres, can be designed to maintain pH neutrality within the hydrogel. Alternatively, antioxidants can be incorporated to stabilize the hydrogel in high-pH environments. Furthermore, intelligent responsive materials can be engineered. For instance, polymers that cause hydrogels to shrink at high temperatures can be introduced to reduce porosity and water penetration. Similarly, hydrogels responsive to ionic strength can be enhanced by adding polyelectrolytes that shrink in high salt environments, thereby inhibiting excessive swelling at extreme pH levels. Through these strategies, SA-based hydrogels can achieve an integrated design of “structure-function-stability” in complex environments, thereby expanding their application potential in biomedicine, flexible electronics, and environmental engineering fields. Overall, for flexible electronics, the primary challenge is related to maintaining electrical conductivity while ensuring mechanical flexibility, stability, and self-healing efficiency. The potential solutions include the incorporation of conductive nanomaterials and the use of multi-layered hydrogel structures to enhance performance.

With the advancement of our knowledge in soft-tissue injury mechanisms and repair processes, SA-based hydrogels are getting more attention in tissue engineering. In tissue engineering, one of the key challenges is achieving optimal biocompatibility and controlled degradation rates. Some strategies, such as the use of bioactive molecules and tailored cross-linking techniques, could be beneficial to address these issues. Existing research has highlighted strategies for optimizing the degradation rate of SA-based hydrogels, primarily through functionalization methods such as oxidation or sulfation. Periodate oxidation introduces aldehyde groups,

forming dynamic Schiff base bonds that confer pH-responsive degradation capabilities. Alternatively, sulfation of SA enhances hydrophilicity and negative charge density, promoting interaction with endogenous enzymes such as lysozyme and accelerating enzymatic hydrolysis. To further refine degradation strategies, ion cross-linking regulation can be employed. For instance, a mixture of Ca^{2+} (strong cross-linking) and Mg^{2+} (weak cross-linking) ions allows graded degradation through ion competition and displacement.

Ion chelator loading is another approach, where ethylenediaminetetraacetic acid microspheres encapsulated within the SA hydrogel gradually diffuse and chelate Ca^{2+} , actively regulating the network disintegration rate. Simultaneously, a dynamic match between degradation and regeneration can be engineered. Gradient degradation structures can be designed to form a layered structure with local cross-linking density regulated via 3D printing parameters. This structure features rapid outer layer degradation (aligning with epidermal regeneration) and slower inner layer degradation (supporting dermal repair). Cellular involvement in degradation regulation is also a viable design method. For example, hydrogels loaded with MSCs leverage the cells' secretions to degrade the surrounding matrix, creating a “cell-guided” degradation-regeneration coupling pathway. Ultimately, real-time monitoring of the regeneration process and degradation triggering can be achieved by designing biosensors. Embedding pH or reactive oxygen species-sensitive fluorescent probes within the hydrogel allows for the continuous monitoring of the regeneration process and the timely initiation of degradation. On the other hand, advanced manufacturing is an effective way to solve personalized tissue engineering applications. 3D bioprinting has allowed us to prepare 3D tissues with the right shapes and a mix of ingredients that imitate real tissue. This is a potential paradigm shift for making workable tissue organs, paving the way for printing soft tissue constructs to be used *in vivo*. Lately, there's been an increase in research into 3D bioprinting of soft tissues, and the results are encouraging, pushing the field ahead. The

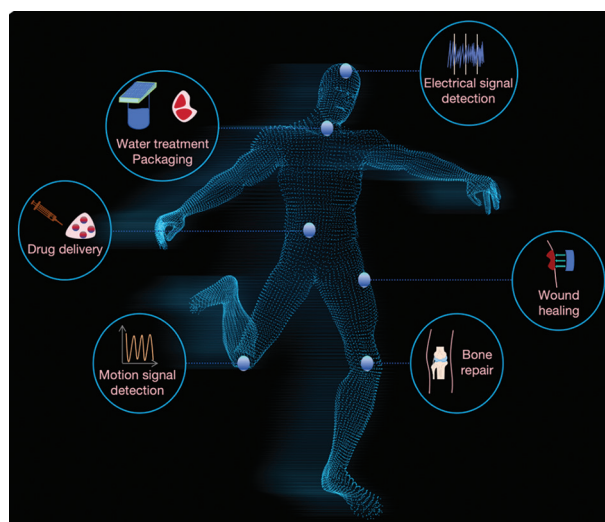


Figure 7. Future prospects of sodium alginate-based hydrogels. Image created by the authors from Freepik.com.

Advances in sodium alginate-based hydrogels

core challenges faced by high-precision 3D printing at present are mainly the following three aspects:

- (i) The contradiction between rheological properties and extrudability. The low viscosity of SA hydrogel can easily lead to the collapse of the printing structure, whereas the high viscosity is difficult to extrude
- (ii) The cross-linking and forming speeds are not matched, and the traditional ion cross-linking speed is slow, which affects the accuracy of layer-by-layer stacking
- (iii) Resolution limitations, nozzle diameter, extrusion pressure, and other parameters limit the formability of microstructures ($<100\ \mu\text{m}$).

In addition, physical modification methods can be used to adjust their rheological properties, such as adding nanoclay and cellulose nanocrystals. Meanwhile, functionalization can also be used to endow ink with self-healing ability, reducing extrusion breakage. The existing research also has many faster and more efficient cross-linking methods, such as photocuring and introducing photosensitive groups to modify SA-based hydrogels, which can achieve second-level curing and support structure. Finally, optimizing printing process parameters requires corresponding optimization of the nozzle diameter, pressure, printing speed, and temperature control of the printer to ensure the accuracy of 3D printing. Artificial intelligence models can also predict the relationship between ink rheology, printing parameters, and structural accuracy, achieving intelligent control. However, significant challenges remain before we can produce fully integrated, functional organs suitable for clinical use. Natural soft tissues are complicated arrangements of different cell types and the ECM, where the organization of cells, matrix components, growth factors, and their interactions presents a significant challenge. To engineer artificial tissues and organs that work, the bio-inks used in bioprinting are now incorporating a cocktail of components and cell types. Consequently, a key research focus is on precisely assembling these diverse elements following the anatomical blueprint of natural tissues, ensuring that the spatial architecture supports the necessary interactions between components.

In terms of water treatment, the stability and water resistance of SA-based hydrogel are poor, making it unable to meet the application's needs. In practical applications, it is usually necessary to improve its stability and water resistance through further processing or modification. SA-based hydrogels typically have a dense pore structure and low specific surface area, which is not conducive to their adsorption performance for pollutants. Therefore, enhancing SA-based hydrogels' porosity and active adsorption sites is crucial for improving performance. In addition, the efficacy of SA-based hydrogels is significantly influenced by environmental conditions, particularly pH levels. In acidic environments, SA-based hydrogel spheres are prone to structural degradation, adversely affecting their adsorption efficiency and recyclability. Importantly, while SA-based hydrogels exhibit notable adsorption capabilities for individual dyes or heavy metal ions, their performance is suboptimal when treating industrial wastewater with complex compositions. Furthermore, although SA-based

hydrogels and their derivatives possess regenerative and recyclable properties, their regeneration efficiency and economic viability in industrial applications require further research and optimization.

The 3D network structure of SA-based hydrogels can regulate their mechanical properties and dynamic response behavior through ionic cross-linking, covalent cross-linking, or composite coagulation. For example, their ionic sensitivity enables reversible swelling/shrinking in response to changes in pH, ion concentration, or electric field, aligning well with the design requirements of intelligent perception feedback systems. In flexible sensors, these hydrogels can generate electrical signals (such as piezoresistive effects) through deformation, providing real-time environmental data for artificial intelligence equipment. Thus, SA-based hydrogels offer numerous potential integration points with artificial intelligence hardware. Combining artificial intelligence and machine learning technologies to optimize the performance of SA-based hydrogels represents a cutting-edge research direction in material science and bioengineering. These hydrogels are widely used in drug delivery, tissue engineering, and flexible sensors due to their biocompatibility, degradability, and controllable physical and chemical properties. Traditional optimization methods rely on experimental trial and error, while artificial intelligence and machine learning can accelerate the optimization of key properties.

- (i) Mechanical performance regulation: Neural networks can predict the effects of different formulations (such as Ca^{2+} concentration and SA molecular weight) on mechanical properties, reducing the number of experimental iterations
- (ii) Dynamic response performance: Supervised learning can analyze the non-linear relationship between response parameters (such as swelling rate) and environmental variables (ion concentration and temperature)
- (iii) Functionalization improvement: Graph neural networks can predict interactions between functional molecules and SA, accelerating candidate molecule screening.

In future development, SA-based hydrogels can integrate molecular simulation (atomic scale), experimental data (macro scale), and clinical needs (application scale) to build multi-level artificial intelligence models, overcoming single-scale optimization limitations. Simultaneously, integrating a robotic experimental platform, real-time representation, and online machine learning models can achieve a "design-synthesis-testing-optimization" closed loop, reducing the research and development cycle by over 90%. Intelligent hydrogels embedded with artificial intelligence algorithms can dynamically adjust drug release rates or mechanical stiffness based on real-time feedback from environmental signals via built-in sensors (such as flexible electronics). Finally, based on patient-specific data (such as tissue hardness and inflammatory factor levels), machine learning models can be trained to customize personalized hydrogel scaffolds, combining 3D bioprinting technology to achieve precise medical treatments.

Due to their biocompatibility, biodegradability, and gel-forming properties, SA-based hydrogels are emerging as

promising materials in food packaging. Research demonstrates that these hydrogels can extend the shelf life of food products and reduce environmental waste, attributed to their unique permeability, moisture regulation, and biodegradability. However, despite significant advancements in the application of SA-based hydrogels for food packaging, several challenges remain. A key challenge among these is optimizing the balance between film-forming capability and decomposition rate. Expanding the range of compatible edible materials is essential for broader application.

In the field of MEG, SA-based hydrogels have shown some progress, yet several limitations persist. For instance, the power output, including current density and voltage, remains relatively low, restricting their energy harvesting efficiency in practical scenarios. Moreover, while these hydrogels can absorb ambient moisture, their stability and adaptability under varying temperature and humidity conditions require enhancement to ensure reliable performance in diverse environments. Future research should focus on these aspects to facilitate widespread adoption in real-world applications.

In summary, SA-based hydrogels have distinctive properties and are increasingly explored across various fields. However, numerous scientific challenges remain unresolved. Targeted and in-depth research is essential to advance the fundamental understanding and practical applications of SA-based hydrogels, fostering their development and utilization in diverse domains.

5. Limitations

While this paper comprehensively reviews SA-based hydrogels and their applications, several limitations should be acknowledged. First, the review may not fully explore emerging functionalization techniques, such as bio-inspired or biomimetic approaches, which could further enhance the properties of these hydrogels. This gap limits exploring innovative strategies that could significantly advance their functional capabilities. Second, the analysis of applications, although broad, lacks in-depth discussions on specific challenges and solutions for each field. For instance, detailed long-term stability and degradation studies are crucial for predicting hydrogel performance over time, especially in biomedical and environmental applications, but these aspects are not extensively covered. Finally, the paper does not delve into the economic feasibility and scalability of the functionalization methods discussed. Understanding the cost-benefit and scalability of these methods is essential for translating laboratory findings into practical industrial and clinical applications. Addressing these limitations in future research could provide a more complete understanding of SA-based hydrogels and their potential for innovation and practical use.

6. Conclusions

SA-based hydrogels have distinctive properties and are extensively explored across various fields. Their potential applications span from biomedical engineering to environmental management, showcasing their versatility

and adaptability. In the biomedical field, these hydrogels hold promise for rehabilitation detection, tissue engineering, drug delivery, and wound healing. In environmental management, they can be utilized for water treatment and pollution control. However, numerous scientific challenges remain unresolved. For instance, optimizing the mechanical properties of these hydrogels through multimethod functionalization to meet specific application requirements, combining with artificial intelligence, enhancing their biocompatibility for *in vivo* use, and improving their degradation rates to ensure environmental sustainability are areas that require further investigation. Targeted and in-depth research is essential to advance the fundamental understanding and practical applications of SA-based hydrogels. By addressing these challenges, we can foster their development and utilization in diverse domains, ultimately contributing to advancements in healthcare, environmental protection, and beyond.

Acknowledgement

None.

Financial support

This work is supported by the National Natural Science Foundation of China (Grant No. 52405315, No. 42176130), Shandong Provincial Natural Science Foundation (ZR2024QE197), the Research Start-up Funds for Recruited Talents of University of Health and Rehabilitation Sciences (KWXXZ 2023026) and Funded with the Marine Natural Products R&D Laboratory, Qingdao Key Laboratory (QDSHYTRCWYJKF 2024-01).

Conflicts of interest statement

The authors declare no competing interests.

Author contributions

Conceptualization: ZM and XW; Writing – original draft: ZM and XW; Writing – review & editing: YH, KT, JM, and YF. All authors read and approved the final version of the manuscript.

Ethics approval and consent to participate

Not applicable.

Consent for publication

Not applicable.

Availability of data

Not applicable.

Open access statement

This is an open-access journal, and articles are distributed under the terms of the Creative Commons Attribution-Non-Commercial-Share Alike 4.0 License, which allows others to remix, tweak, and build upon the work non-commercially if appropriate credit is given. The new creations are licensed under identical terms.

References

1. Taylor DL, In Het Panhuis M. Self-healing hydrogels. *Adv Mater.* 2016;28(41):9060-9093. doi: 10.1002/adma.201601613
2. Li X, Gong JP. Design principles for strong and tough hydrogels. *Nat Rev Mater.* 2024;9(6):380-398. doi: 10.1038/s41578-024-00672-3
3. Ji D, Park JM, Oh MS, et al. Superstrong, superstiff, and conductive alginate hydrogels. *Nat Commun.* 2022;13(1):3019. doi: 10.1038/s41467-022-30691-z
4. Abdul Khalil HPS, Lai TK, Tye YY, et al. A review of extractions of seaweed hydrocolloids: Properties and applications. *Express Polym Lett.* 2018;12(4):296-317. doi: 10.3144/expresspolymlett.2018.27
5. Liu GW, Pickett MJ, Kuosmanen JLP, et al. Drinkable *in situ*-forming tough hydrogels for gastrointestinal therapeutics. *Nat Mater.* 2024;23:1292-1999. doi: 10.1038/s41563-024-01811-5

6. Luo R, Liu J, Cheng Q, Shionoya M, Gao C, Wang R. Oral microsphere formulation of M2 macrophage-mimetic Janus nanomotor for targeted therapy of ulcerative colitis. *Sci Adv.* 2024;10(26):ead06798. doi: 10.1126/sciadv.ad06798
7. Zhao M, Kang M, Wang J, et al. Stem cell-derived nanovesicles embedded in dual-layered hydrogel for programmed ROS regulation and comprehensive tissue regeneration in burn wound healing. *Adv Mater.* 2024;36(32):2401369. doi: 10.1002/adma.202401369
8. Guo R, Li X, Zhou Y, et al. Semi-liquid metal-based highly permeable and adhesive electronic skin inspired by spider web. *Sci Bull (Beijing).* 2024;69(17):2723-2734. doi: 10.1016/j.scib.2024.06.032
9. Wang M, Zhang X, Liu B, et al. Immunotherapeutic hydrogel with photothermal induced immunogenic cell death and STING Activation for post-surgical treatment. *Adv Funct Mater.* 2023;33(29):2300199. doi: 10.1002/adfm.202300199
10. Yan J, Zhou T, Peng J, Wang H, Jiang L, Cheng Q. Sustainable liquid metal-induced conductive nacre. *Sci Bull.* 2024;69(7):913-921. doi: 10.1016/j.scib.2024.01.033
11. Jiang XY, Li L, Yan JN, et al. Characterization of hydrogel beads constructed from gelatinized lotus rhizome starch and sodium alginate by calcium cross-linking. *Food Hydrocoll.* 2024;154:110102. doi: 10.1016/j.foodhyd.2024.110102
12. Hui Z, Zhang Z, Wang Y, et al. Gradiently foaming ultrasoft hydrogel with stop holes for highly deformable, crack-resistant and sensitive conformal human-machine interfaces. *Adv Mater.* 2024;36(23):2314163. doi: 10.1002/adma.202314163
13. Lei XX, Hu JJ, Zou CY, et al. Multifunctional two-component *in-situ* hydrogel for esophageal submucosal dissection for mucosa uplift, postoperative wound closure and rapid healing. *Bioact Mater.* 2023;27:461-473. doi: 10.1016/j.bioactmat.2023.04.015
14. Liang L, Hou T, Ouyang Q, et al. Antimicrobial sodium alginate dressing immobilized with polydopamine-silver composite nanospheres. *Compos Part B Eng.* 2020;188:107877. doi: 10.1016/j.compositesb.2020.107877
15. Fan X, Huang J, Zhang W, et al. A multifunctional, tough, stretchable, and transparent curcumin hydrogel with potent antimicrobial, antioxidative, anti-inflammatory, and angiogenesis capabilities for diabetic wound healing. *ACS Appl Mater.* 2024;16(8):9749-9767. doi: 10.1021/acsami.3c16837
16. Raj V, Raorane CJ, Shastri D, Kim SC, Lee S. Engineering a self-healing grafted chitosan-sodium alginate based hydrogel with potential keratinocyte cell migration property and inhibitory effect against fluconazole resistance *Candida albicans* biofilm. *Int J Biol Macromol.* 2024;261:129774. doi: 10.1016/j.ijbiomac.2024.129774
17. Solano AG, Dupuy J, Therriault H, et al. An alginate-based macroporous hydrogel matrix to trap cancer cells. *Carbohydr Polym.* 2021;266:118115. doi: 10.1016/j.carbpol.2021.118115
18. Sun J, Tan H. Alginate-based biomaterials for regenerative medicine applications. *Mater (Basel).* 2013;6(4):1285-1309. doi: 10.3390/ma6041285
19. Wei Q, Zhou J, An Y, Li M, Zhang J, Yang S. Modification, 3D printing process and application of sodium alginate based hydrogels in soft tissue engineering: A review. *Int J Biol Macromol.* 2023;232:123450. doi: 10.1016/j.ijbiomac.2023.123450
20. Lee DU, Kayumov M, Park J, et al. Antibiofilm and antithrombotic hydrogel coating based on superhydrophilic zwitterionic carboxymethyl chitosan for blood-contacting devices. *Bioact Mater.* 2024;34:112-124. doi: 10.1016/j.bioactmat.2023.12.009
21. Song R, Wang X, Johnson M, et al. Enhanced strength for double network hydrogel adhesive through cohesion-adhesion balance. *Adv Funct Mater.* 2024;34(23):2313322. doi: 10.1002/adfm.202313322
22. Zhang G, Wang X, Meng G, et al. Enzyme-mineralized PVASA hydrogels with combined toughness and strength for bone tissue engineering. *ACS Appl Mater.* 2023;16(1):178-189. doi: 10.1021/acsami.3c14006
23. Zhang B, Cai X, Li J, et al. Biocompatible and stable quasi-solid-state zinc-ion batteries for real-time responsive wireless wearable electronics. *Energ Environ Sci.* 2024;17(11):3878-3887. doi: 10.1039/d4ee01212g
24. Zhuo F, Zhou J, Liu Y, et al. Kirigami-inspired 3D-printable MXene organohydrogels for soft electronics. *Adv Funct Mater.* 2023;33(52):2308487. doi: 10.1002/adfm.202308487
25. Wei L, Wang X, Fu J, Yin J, Hu J. A physically cross-linked double network polysaccharides/Ca²⁺ hydrogel scaffold for skeletal muscle tissue engineering. *Colloid Surface A.* 2023;668:131410. doi: 10.1016/j.colsurfa.2023.131410
26. Peng G, Hu J, Guo J, et al. Injectable exosome-loaded quaternized chitosan/oxidized sodium alginate hydrogel with self-healing, bioadhesive, and antibacterial properties for treating combined radiation-wound injury. *Chem Eng J.* 2024;494:152933. doi: 10.1016/j.cej.2024.152933
27. Yang X, Huang C, Wang H, et al. Multifunctional nanoparticle-loaded injectable alginate hydrogels with deep tumor penetration for enhanced chemo-immunotherapy of cancer. *ACS Nano.* 2024;18(28):18604-18621. doi: 10.1021/acsnano.4c04766
28. Jiang S, Jing H, Zhuang Y, et al. BMSCs-laden mechanically reinforced bioactive sodium alginate composite hydrogel microspheres for minimally invasive bone repair. *Carbohydr Polym.* 2024;332:121933. doi: 10.1016/j.carbpol.2024.121933
29. Wu M, Liu H, Li D, et al. Smart-responsive multifunctional therapeutic system for improved regenerative microenvironment and accelerated bone regeneration via mild photothermal therapy. *Adv Sci.* 2023;11(2):2304641. doi: 10.1002/advs.202304641
30. Yu J, Yun J, Zhang S, et al. Hydrogel fiber fabric combining rapid water transport, thermal localization, and large-scale production for ultra-high salt-resistant solar desalination. *Nano Energy.* 2023;117:108847. doi: 10.1016/j.nanoen.2023.108847
31. Hadi A, Nawab A, Alam F, Naqvi S. Development of sodium alginate-aloe vera hydrogel films enriched with organic fibers: Study of the physical, mechanical, and barrier properties for food-packaging applications. *Sustain Food Technol.* 2023;1(6):863-873. doi: 10.1039/d3fb00122a
32. Huang Z, Li C, Ying W, et al. A hydrogel-based moist-electric generator with superior energy output and environmental adaptability. *Nano Energy.* 2024;126:109673. doi: 10.1016/j.nanoen.2024.109673
33. Zhang Y, Li S, Gao Z, et al. Highly conductive and tough polyacrylamide/sodium alginate hydrogel with uniformly distributed polypyrrole nanospheres for wearable strain sensors. *Carbohydr Polym.* 2023;315:120953. doi: 10.1016/j.carbpol.2023.120953
34. Ge J, Fang C, Tan H, et al. Endogenous zinc-ion-triggered *in situ* gelation enables zn capture to reprogram benign hyperplastic prostate microenvironment and shrink prostate. *Adv Mater.* 2023;36(11):2307796. doi: 10.1002/adma.202307796
35. Maihemuti A, Zhang H, Lin X, et al. 3D-printed fish gelatin scaffolds for cartilage tissue engineering. *Bioact Mater.* 2023;26:77-87. doi: 10.1016/j.bioactmat.2023.02.007
36. Shen W, Pei P, Zhang C, et al. A polymeric hydrogel to eliminate programmed death-ligand 1 for enhanced tumor radio-immunotherapy. *ACS Nano.* 2023;17(23):23998-24011. doi: 10.1021/acsnano.3c08875
37. Ren C, Zhong D, Qi Y, et al. Bioinspired pH-responsive microalgal hydrogels for oral insulin delivery with both hypoglycemic and insulin sensitizing effects. *ACS Nano.* 2023;17(14):14161-14175. doi: 10.1021/acsnano.3c04897
38. Ma J, Li S, Li X, Guo K, Wang H, Yin J. Facile fabrication of liquid metal enabled conductive zwitterionic hydrogel for robust electrochemical sensing in complex serum. *Chem Eng J.* 2024;492:152433. doi: 10.1016/j.cej.2024.152433
39. Jin F, Liao S, Li W, et al. Amphiphilic sodium alginate-polylysine hydrogel with high antibacterial efficiency in a wide pH range. *Carbohydr Polym.* 2023;299:120195.

- doi: 10.1016/j.carbpol.2022.120195
40. Lu J, Song J, Zhang P, et al. Biomaterialized polydopamine nanoparticle-based sodium alginate hydrogels for delivery of anti-serine/threonine protein kinase B-rapidly accelerated fibrosarcoma siRNA for metastatic melanoma therapy. *ACS Nano*. 2023;17(18):18318-18331. doi: 10.1021/acsnano.3c05563
 41. Qi Z, Ren R, Hu J, et al. Flexible supercapacitor with wide electrochemical stable window based on hydrogel electrolyte. *Small*. 2024;20(30):e2400369. doi: 10.1002/smll.202400369
 42. Choi G, An SH, Choi JW, et al. Injectable alginate-based *in situ* self-healable transparent hydrogel as a vitreous substitute with a tamponading function. *Biomaterials*. 2024;305:122459. doi: 10.1016/j.biomaterials.2023.122459
 43. Liu C, Mao Y, Jiang L, et al. Large strain, tissue-like and self-healing conductive double-network hydrogel for underwater information transmission. *Chem Eng J*. 2024;482:148863. doi: 10.1016/j.cej.2024.148863
 44. Zhang J, Yan K, Huang J, et al. Mechanically robust, flexible, fast responding temperature sensor and high-resolution array with ionically conductive double cross-linked hydrogel. *Adv Funct Mater*. 2024;34(21):2314433. doi: 10.1002/adfm.202314433
 45. Hu X, He J, Qiao L, et al. Multifunctional dual network hydrogel loaded with novel tea polyphenol magnesium nanoparticles accelerates wound repair of MRSA infected diabetes. *Adv Funct Mater*. 2024;34(22):2312140. doi: 10.1002/adfm.202312140
 46. Zhang M, Feng Q, Zhang G, et al. Calcium-capturing hydrogel with self-reinforced multi-dynamic networks for effective periodontal bone regeneration in three-dimension. *Adv Funct Mater*. 2025;35(12):2415185. doi: 10.1002/adfm.202415185
 47. Li H, Xia Y, Guo R, et al. Direct-ink-writable nanocellulose ternary hydrogels via one-pot gelation with alginate and calcium montmorillonite. *Carbohydr Polym*. 2024;344:122494. doi: 10.1016/j.carbpol.2024.122494
 48. Mahmood A, Sharif A, Muhammad F, et al. Development and *in vitro* evaluation of (β -cyclodextrin-g-methacrylic acid)/Na⁺-montmorillonite nanocomposite hydrogels for controlled delivery of lovastatin. *Int J Nanomed*. 2019;14:5397-5413. doi: 10.2147/ijn.S209662
 49. Li W, Tao LQ, Kang MC, et al. Tunable mechanical, self-healing hydrogels driven by sodium alginate and modified carbon nanotubes for health monitoring. *Carbohydr Polym*. 2022;295:119854. doi: 10.1016/j.carbpol.2022.119854
 50. Zhang R, Wu C, Yang W, et al. Design of delignified wood-based high-performance composite hydrogel electrolyte with double crosslinking of sodium alginate and PAM for flexible supercapacitors. *Ind Crop Prod*. 2024;210:118187. doi: 10.1016/j.indcrop.2024.118187
 51. Seifi S, Shamloo A, Barzoki AK, et al. Engineering biomimetic scaffolds for bone regeneration: Chitosan/alginate/polyvinyl alcohol-based double-network hydrogels with carbon nanomaterials. *Carbohydr Polym*. 2024;339:122232. doi: 10.1016/j.carbpol.2024.122232
 52. Catoira MC, Fusaro L, Di Francesco D, Ramella M, Boccafocchi F. Overview of natural hydrogels for regenerative medicine applications. *J Mater Sci Mater M*. 2019;30(10):115. doi: 10.1007/s10856-019-6318-7
 53. Zhang X, Liu Y, Wang Z, et al. pH-responsive and self-adaptive injectable sodium alginate/carboxymethyl chitosan hydrogel accelerates infected wound healing by bacteriostasis and immunomodulation. *Carbohydr Polym*. 2025;354:123322. doi: 10.1016/j.carbpol.2025.123322
 54. Qin BQ, Wu SZ, Nie R, et al. SDF-1 α /BMP-12 loaded biphasic sustained-release SIS hydrogel/SA microspheres composite for tendon regeneration. *Biomaterials*. 2025;320:123246. doi: 10.1016/j.biomaterials.2025.123246
 55. Zhang D, Hu Z, Hao R, et al. Fabrication and hemostasis evaluation of a carboxymethyl chitosan/sodium alginate/Resina draconis composite sponge. *Int J Biol Macromol*. 2024;274:133265. doi: 10.1016/j.ijbiomac.2024.133265
 56. Zhang Y, Guo D, Shen X, Tang Z, Lin B. Recoverable and degradable carboxymethyl chitosan polyelectrolyte hydrogel film for ultra stable encapsulation of curcumin. *Int J Biol Macromol*. 2024;268:131616. doi: 10.1016/j.ijbiomac.2024.131616
 57. Xu J, Song W, Ren L, et al. Reinforced hydrogel building via formation of alginate-chitosan double network with pH and salt-responsiveness and electric conductivity for soft actuators. *Int J Biol Macromol*. 2024;263:130282. doi: 10.1016/j.ijbiomac.2024.130282
 58. Ding S, Jin X, Guo J, et al. A biomimetic asymmetric structured intelligent wound dressing with dual-modality humidity-pressure sensing for non-invasive and real-time wound healing monitoring. *Adv Fiber Mater*. 2024;7:156-171. doi: 10.1007/s42765-024-00473-x
 59. Wei T, Zhao R, Fang L, et al. Encoded magnetization for programmable soft miniature machines by covalent assembly of modularly coupled microgels. *Adv Funct Mater*. 2023;34(16):2311908. doi: 10.1002/adfm.202311908
 60. Lou Y, Wang J, Peng Y, et al. Double network hydrogel confined MXene/Liquid metal by dynamic hydrogen bond for high-performance wearable sensors. *Chem Eng J*. 2024;500:156884. doi: 10.1016/j.cej.2024.156884
 61. Jiang Y, Guo S, Jiao J, Li L. A biphasic hydrogel with self-healing properties and a continuous layer structure for potential application in osteochondral defect repair. *Polymers*. 2023;15(12):2744. doi: 10.3390/polym15122744
 62. Öztürk E, Stauber T, Levinson C, Cavalli E, Arlov Ø, Zenobi-Wong M. Tyrosinase-crosslinked, tissue adhesive and biomimetic alginate sulfate hydrogels for cartilage repair. *Biomater*. 2020;15(4):045019. doi: 10.1088/1748-605X/ab8318
 63. Qiao L, Liang Y, Chen J, et al. Antibacterial conductive self-healing hydrogel wound dressing with dual dynamic bonds promotes infected wound healing. *Bioact Mater*. 2023;30:129-141. doi: 10.1016/j.bioactmat.2023.07.015
 64. Yang JS, Xie YJ, He W. Research progress on chemical modification of alginate: A review. *Carbohydr Polym*. 2011;84(1):33-39. doi: 10.1016/j.carbpol.2010.11.048
 65. Geng H, Zheng X, Zhang Y, et al. Microenvironment-responsive hydrogels with detachable skin adhesion and mild-temperature photothermal property for chronic wound healing. *Adv Funct Mater*. 2023;33(51):2305154. doi: 10.1002/adfm.202305154
 66. Zhang J, Zhang S, Liu C, et al. Photopolymerized multifunctional sodium alginate-based hydrogel for antibacterial and coagulation dressings. *Int J Biol Macromol*. 2024;260:129428. doi: 10.1016/j.ijbiomac.2024.129428
 67. El-Sayed NS, Hashem AH, Khattab TA, Kamel S. New antibacterial hydrogels based on sodium alginate. *Int J Biol Macromol*. 2023;248:125872. doi: 10.1016/j.ijbiomac.2023.125872
 68. Chen T, Qian Q, Makvandi P, et al. Engineered high-strength biohydrogel as a multifunctional platform to deliver nucleic acid for ameliorating intervertebral disc degeneration. *Bioact Mater*. 2023;25:107-121. doi: 10.1016/j.bioactmat.2023.01.010
 69. Li M, Tian J, Yu K, et al. A ROS-responsive hydrogel incorporated with dental follicle stem cell-derived small extracellular vesicles promotes dental pulp repair by ameliorating oxidative stress. *Bioact Mater*. 2024;36:524-540. doi: 10.1016/j.bioactmat.2024.06.036
 70. Li Y, Tian Z, Gao XZ, et al. All-weather self-powered intelligent traffic monitoring system based on a conjunction of self-healable piezoresistive sensors and triboelectric nanogenerators. *Adv Funct Mater*. 2023;33(52):2308845. doi: 10.1002/adfm.202308845
 71. Zhang MD, Huang X, Li Z, et al. White-light-induced synthesis of injectable alginate-based composite hydrogels for rapid hemostasis. *Mil Med Res*. 2023;10(1):47. doi: 10.1186/s40779-023-00483-7
 72. Yan X, Zhao R, Lin H, Bao X, Zhao Z, Song S. Dual-network conductive hydrogel with rapid self-healing ability and great fatigue

- resistance as strain sensor for human motion monitoring. *Eur Polym J*. 2023;201:112570.
doi: 10.1016/j.eurpolymj.2023.112570
73. Zhang X, Chen S, Ding Z, Chen M. Highly sensitive and high strength hydrogel sensors with interpenetrating network structure for strain-stimulus detection. *Sensory Actua A Phys*. 2023;357:114388.
doi: 10.1016/j.sna.2023.114388
 74. Jiang L, Dong X, Chen L, et al. A composite hydrogel membrane with shape and water retention for corneal tissue engineering. *Heliyon*. 2023;9(7):e17950.
doi: 10.1016/j.heliyon.2023.e17950
 75. Gao LT, Chen YM, Aziz Y, et al. Tough, self-healing and injectable dynamic nanocomposite hydrogel based on gelatin and sodium alginate. *Carbohydr Polym*. 2024;330:121812.
doi: 10.1016/j.carbpol.2024.121812
 76. Liu S, Bastola AK, Li L. A 3D printable and mechanically robust hydrogel based on alginate and graphene oxide. *ACS Appl Mater Interfaces*. 2017;9(47):41473-41481.
doi: 10.1021/acsami.7b13534
 77. İsmail O, Gökçe Kocabay Ö. Absorption and adsorption studies of polyacrylamide/sodium alginate hydrogels. *Colloid Polym Sci*. 2021;299(5):783-796.
doi: 10.1007/s00396-020-04796-0
 78. Reakasame S, Boccaccini AR. Oxidized alginate-based hydrogels for tissue engineering applications: A review. *Biomacromolecules*. 2017;19(1):3-21.
doi: 10.1021/acs.biomac.7b01331
 79. Zhao X, Xue W, Ding W, et al. A novel injectable sodium alginate/chitosan/sulfated bacterial cellulose hydrogel as biohybrid artificial pancreas for real-time glycaemic regulation. *Carbohydr Polym*. 2025;354:123323.
doi: 10.1016/j.carbpol.2025.123323
 80. Malaeb W, Bahmad HF, Abou-Kheir W, Mhanna R. The sulfation of biomimetic glycosaminoglycan substrates controls binding of growth factors and subsequent neural and glial cell growth. *Biomater Sci*. 2019;7(10):4283-4298.
doi: 10.1039/c9bm00964g
 81. Pettinelli N, Sabando C, Rodríguez-Llamazares S, et al. Sodium alginate-g-polyacrylamide hydrogel for water retention and plant growth promotion in water-deficient soils. *Ind Crop Prod*. 2024;222:119759.
doi: 10.1016/j.indcrop.2024.119759
 82. Yu L, Chen A, Tang R, Zhao F, Li J, Wei L. Multiple hydrogen bonding induced by semi-interpenetrating polymer network binder to enhance the electrochemical performance of sodium-ion batteries electrodes. *Chem Eng J*. 2024;502:158006.
doi: 10.1016/j.cej.2024.158006
 83. López-Díaz A, Vázquez AS, Vázquez E. Hydrogels in soft robotics: Past, present, and future. *ACS Nano*. 2024;18(32):20817-20826.
doi: 10.1021/acsnano.3c12200
 84. Feng C, Xu B, Chen L, Qiu Z, Guo J. Cellulose hydrogels with high response sensitivity and mechanical adaptability for flexible strain sensor and triboelectric nanogenerator. *Eur Polym J*. 2024;214:113173.
doi: 10.1016/j.eurpolymj.2024.113173
 85. Wang W, Yao D, Wang H, et al. A breathable, stretchable, and self-calibrated multimodal electronic skin based on hydrogel microstructures for wireless wearables. *Adv Funct Mater*. 2024;34(32):2316339.
doi: 10.1002/adfm.202316339
 86. Tong R, Ma Z, Gu P, et al. Stretchable and sensitive sodium alginate ionic hydrogel fibers for flexible strain sensors. *Int J Biol Macromol*. 2023;246:125683.
doi: 10.1016/j.ijbiomac.2023.125683
 87. Zhang M, Ren J, Li R, Zhang W, Li Y, Yang W. Multifunctional sodium lignosulfonate/xanthan gum/sodium alginate/polyacrylamide ionic hydrogels composite as a high-performance wearable strain sensor. *Int J Biol Macromol*. 2024;261:129718.
doi: 10.1016/j.ijbiomac.2024.129718
 88. Tang L, Wu P, Zhuang H, et al. Nitric oxide releasing polyvinyl alcohol and sodium alginate hydrogels as antibacterial and conductive strain sensors. *Int J Biol Macromol*. 2023;241:124564.
doi: 10.1016/j.ijbiomac.2023.124564
 89. Xue H, Wang D, Jin M, et al. Hydrogel electrodes with conductive and substrate-adhesive layers for noninvasive long-term EEG acquisition. *Microsyst Nanoeng*. 2023;9(1):79.
doi: 10.1038/s41378-023-00524-0
 90. Zhang D, Sun H, Huang M, et al. Construction of "island-bridge" microstructured conductive coating for enhanced impedance response of organohydrogel strain sensor. *Chem Eng J*. 2024;496:153752.
doi: 10.1016/j.cej.2024.153752
 91. Lan X, Ma Z, Dimitrov A, et al. Double crosslinked hyaluronic acid and collagen as a potential bioink for cartilage tissue engineering. *Int J Biol Macromol*. 2024;273:132819.
doi: 10.1016/j.ijbiomac.2024.132819
 92. Moon SH, Park TY, Cha HJ, Yang YJ. Photo-/thermo-responsive bioink for improved printability in extrusion-based bioprinting. *Mater Today Bio*. 2024;25:100973.
doi: 10.1016/j.mtbio.2024.100973
 93. Boumegnane A, Douhi S, Batine A, et al. Rheological properties and inkjet printability of a green silver-based conductive ink for wearable flexible textile antennas. *Sensors (Basel)*. 2024;24(9):2938.
doi: 10.3390/s24092938
 94. Tóth GS, Backman O, Siivola T, et al. Employing photocurable biopolymers to engineer photosynthetic 3D-printed living materials for production of chemicals. *Green Chem*. 2024;26(7):4032-4042.
doi: 10.1039/d3gc04264b
 95. Norouzi F, Bagheri F, Hashemi-Najafabadi S. Alendronate releasing silk fibroin 3D bioprinted scaffolds for application in bone tissue engineering: Effects of alginate concentration on printability, mechanical properties and stability. *Results Eng*. 2024;22:102186.
doi: 10.1016/j.rineng.2024.102186
 96. Li M, Wang Y, Wei Q, Zhang J, Chen X, An Y. A high-stretching, rapid-self-healing, and printable composite hydrogel based on poly (vinyl alcohol), nanocellulose, and sodium alginate. *Gels*. 2024;10(4):258.
doi: 10.3390/gels10040258
 97. Hui Y, Yao Y, Qian Q, et al. Three-dimensional printing of soft hydrogel electronics. *Nat Electron*. 2022;5(12):893-903.
doi: 10.1038/s41928-022-00887-8
 98. Wang X, Liu X, Bi P, et al. Electrochemically enabled embedded three-dimensional printing of freestanding gallium wire-like structures. *ACS Appl Mater*. 2020;12(48):53966-53972.
doi: 10.1021/acsami.0c16438
 99. Xue T, Wei H, Li F, et al. MicroRNA-Modified DNA hexahedron-induced hepatocyte-like cells integrating 3D printed scaffold for acute liver failure therapy. *Adv Funct Mater*. 2024;34(38):2470222.
doi: 10.1002/adfm.202402339
 100. Yuan Y, Zhang Z, Mo F, et al. A biomaterial-based therapy for lower limb ischemia using Sr/Si bioactive hydrogel that inhibits skeletal muscle necrosis and enhances angiogenesis. *Bioact Mater*. 2023;26:264-278.
doi: 10.1016/j.bioactmat.2023.02.027
 101. Wang L, Fan L, Filppula AM, et al. Dual physiological responsive structural color hydrogel particles for wound repair. *Bioact Mater*. 2025;46:494-502.
doi: 10.1016/j.bioactmat.2025.01.002
 102. Sadeghianmaryan A, Ahmadian N, Wheatley S, et al. Advancements in 3D-printable polysaccharides, proteins, and synthetic polymers for wound dressing and skin scaffolding - a review. *Int J Biol Macromol*. 2024;266:131207.
doi: 10.1016/j.ijbiomac.2024.131207
 103. Aitchison AH, Allen NB, Shaffrey IR, et al. Fabrication of a novel 3D extrusion bioink containing processed human articular cartilage matrix for cartilage tissue engineering. *Bioengineering*. 2024;11(4):329.
doi: 10.3390/bioengineering11040329
 104. Synofzik J, Heene S, Jonczyk R, Blume C. Ink-structuring the future of vascular tissue engineering: A review of the physiological bioink design. *Bio Des Manuf*. 2024;7(2):181-205.
doi: 10.1007/s42242-024-00270-w
 105. Jiao T, Lian Q, Lian W, et al. Properties of collagen/sodium alginate hydrogels for bioprinting of skin models. *JBionic Eng*. 2022;20(1):105-118.
doi: 10.1007/s42235-022-00251-8
 106. Wong KY, Nie Z, Wong MS, Wang Y, Liu J. Metal-drug coordination nanoparticles and hydrogels for enhanced delivery. *Adv Mater*. 2024;36(26):e2404053.

- doi: 10.1002/adma.202404053
107. Xiang H, Wang F, Zhang Q, et al. Endogenous stem cell repair strategy via electromechanical interaction for stress injury. *Chem Eng J.* 2025;507:160575.
doi: 10.1016/j.cej.2025.160575
108. Long X, Wang J, Wang H, et al. Injectable 2D-MoS₂-integrated bioadhesive hydrogel as photothermal-derived and drug-delivery implant for colorectal cancer therapy. *Adv Healthc Mater.* 2025;2404842.
doi: 10.1002/adhm.202404842
109. Hu X, Zhang Z, Wu H, et al. Progress in the application of 3D-printed sodium alginate-based hydrogel scaffolds in bone tissue repair. *Mat Sci Eng C Mater.* 2023;152:213501.
doi: 10.1016/j.bioadv.2023.213501
110. Camarero-Espinosa S, Beeren I, Liu H, et al. 3D niche - inspired scaffolds as a stem cell delivery system for the regeneration of the osteochondral interface. *Adv Mater.* 2024;36(34):2310258.
doi: 10.1002/adma.202310258
111. Huang J, Li A, Liang R, et al. Future perspectives: Advances in bone/cartilage organoid technology and clinical potential. *Biomater Transl.* 2024;5(4):425-443.
doi: 10.12336/biomatertransl.2024.04.007
112. Liu D, Wang X, Gao C, et al. Biodegradable piezoelectric - conductive integrated hydrogel scaffold for repair of osteochondral defects. *Adv Mater.* 2024;36(45):2409400.
doi: 10.1002/adma.202409400
113. Hia EM, Suh IW, Jang SR, Park CH. Magnetically responsive micro-clustered calcium phosphate-reinforced cell-laden microbead sodium alginate hydrogel for accelerated osteogenic tissue regeneration. *Carbohydr Polym.* 2024;346:122666.
doi: 10.1016/j.carbpol.2024.122666
114. Qi X, Li Z, Shen L, et al. Highly efficient dye decontamination via microbial salectan polysaccharide-based gels. *Carbohydr Polym.* 2019;219:1-11.
doi: 10.1016/j.carbpol.2019.05.021
115. Lim JYC, Goh SS, Liow SS, Xue K, Loh XJ. Molecular gel sorbent materials for environmental remediation and wastewater treatment. *Mater Chem A.* 2019;7(32):18759-18791.
doi: 10.1039/c9ta05782j
116. Carrión MG, Corripio MAR, Contreras JVH, Marrón MR, Olán GM, Cázares ASH. Optimization and characterization of taro starch, nisin, and sodium alginate-based biodegradable films: Antimicrobial effect in chicken meat. *Poult Sci.* 2023;102:103100.
doi: 10.1016/j.psj.2023.103100
117. Luo C, Guo A, Zhao Y, Sun X. A high strength, low friction, and biocompatible hydrogel from PVA, chitosan and sodium alginate for articular cartilage. *Carbohydr Polym.* 2022;286:119268.
doi: 10.1016/j.carbpol.2022.119268
118. Yue H, Shang Z, Xu P, Feng D, Li X. Preparation of EDTA modified chitooligosaccharide/sodium alginate/Ca²⁺ physical double network hydrogel by using of high-salinity oilfield produced water for adsorption of Zn²⁺, Ni²⁺ and Mn²⁺. *Sep Purif Technol.* 2022;280:119767.
doi: 10.1016/j.seppur.2021.119767
119. Berg J, Seiffert S. Composite hydrogels based on calcium alginate and polyethyleneimine for wastewater treatment. *J Polym Sci.* 2023;61(18):2203-2222.
doi: 10.1002/pol.20230215
120. Dalei G, Das SK, Mohapatra SS, Das S. *In situ* crosslinked Schiff base biohydrogels containing Carica papaya peel extract: Application in the packaging of fresh berries. *Sustain Food Technol.* 2023;1(6):906-920.
doi: 10.1039/d3fb00096f
121. An N, Zhou W. Sodium alginate/ager colourimetric film on porous substrate layer: Potential in intelligent food packaging. *Food Chem.* 2024;445:138790.
doi: 10.1016/j.foodchem.2024.138790
122. Yu K, Yang L, Zhang S, Zhang N. Strong, tough, high-release, and antibacterial nanocellulose hydrogel for refrigerated chicken preservation. *Int J Biol Macromol.* 2024;264:130727.
doi: 10.1016/j.ijbiomac.2024.130727
123. Yu K, Yang L, Zhang S, et al. Soy hull nanocellulose enhances the stretchability, transparency and ionic conductance of sodium alginate hydrogels and application in beef preservation. *Food Hydrocoll.* 2024;152:109938.
doi: 10.1016/j.foodhyd.2024.109938
124. Duan W, Shao B, Wang Z, et al. Silicon nanowire/ionic hydrogel-based hybrid moist-electric generators with enhanced voltage output and operational stability. *Energ Environ Sci.* 2024;17(11):3788-3796.
doi: 10.1039/d4ee00171k
125. Sun J, Ni F, Gu J, et al. Entangled mesh hydrogels with macroporous topologies via cryogelation for rapid atmospheric water harvesting. *Adv Mater.* 2024;36(27):2314175.
doi: 10.1002/adma.202314175

Received: February 12, 2025

Revised: March 23, 2025

Accepted: March 24, 2025

Available online: May 8, 2025